Catena 127 (2015) 222–239

Contents lists available at ScienceDirect

Catena

journal homepage: www.elsevier.com/locate/catena

Chronosequence development and soil variability from a variety of sub-alpine, post-glacial landforms and deposits in the southeastern San Juan Mountains of Colorado

Bradley G. Johnson [a,*], Anthony L. Layzell [b], Martha Cary Eppes [c]

[a] Davidson College, Environmental Studies, 209 Ridge Rd., Davidson, NC 28036, USA
[b] Kansas Geological Survey, University of Kansas, Lawrence, KS 66047, USA
[c] Department of Geography and Earth Sciences, University of North Carolina — Charlotte, McEniry 324, 9201 University City Blvd., Charlotte, NC 28223, USA

ARTICLE INFO

Article history:
Received 17 July 2014
Received in revised form 16 December 2014
Accepted 20 December 2014
Available online xxxx

Keywords:
Chronosequence
Extractable iron
Post-glacial
San Juan Mountains
Parent material
Variability
Sub-alpine

ABSTRACT

Surficial processes acting on post-glacial alpine and sub-alpine landscapes vary at small temporal and spatial scales and are thus often difficult to conceptualize in the context of large-scale landscape evolution models. Soils developing in this setting can thus provide valuable information about landform genesis, sedimentology and age. Relatively few post-glacial chronosequences have been examined in these settings however, particularly for the variety of landforms and parent materials that exist within alpine and sub-alpine environments. Here, we examine a chronosequence of relatively young, post-glacial landforms with varying parent materials and climate histories. We dug and described 39 soil pits in the upper Conejos River Valley of Colorado on a variety of deposits and landforms, including alluvial fans, terraces, colluvium, glacial till, and terminal moraines, and compared soil properties with radiocarbon ages from the area. Our results suggest that some typical chronosequence soil properties (e.g., pH, structure, color) do not correlate with time over short time scales. However, extractable iron ratios (Fe_o/Fe_d) show a relatively strong correlation with age across late-Pleistocene and Holocene time scales and maximum profile clay content shows a weak but statistically significant relationship with age. Both of these trends are stronger when examined across a single parent material. Differences in initial parent material texture and dust inputs seem to be the most significant complicating factors over post-glacial time scales. Soil property development through time is most inconsistent in cumulic alluvial fan soils. This observation may indicate that alluvial fans are more responsive to sub-basin scale processes as opposed to fluvial terraces that are more likely respond to processes active across the entire basin. These differences would explain why stratigraphically similar alluvial fans are mantled by soils with varying development. Nonetheless, horizonation, clay content, and extractable iron ratios provide a useful tool for correlating young deposits, assigning ages, and interpreting the geomorphic history of complex post-glacial environments.

1. Introduction

Accurate chronologies are key elements of geomorphic mapping and the interpretation of surface morphology. Soil chronosequences have long been used to provide inexpensive relative ages of landforms and deposits, which in turn allows for the investigation of landscape evolution where numerical age dating is limited. In addition, soils can yield important information relating to incision and sedimentation rates (e.g., Birkeland et al., 2003; Leigh and Webb, 2006), landscape response to climate change and anthropogenic impacts (Eppes et al., 2008; Johnson et al., 2013; Layzell et al., 2012b, e.g., McFadden and McAuliffe, 1997), as well as alluvial response to intrinsic variability (Eppes and McFadden, 2008). Despite their importance as tools for investigating and reconstructing the geomorphic history of landscapes, few soil chronosequences have been created for the post-last glacial maximum (LGM) deposits of alpine and sub-alpine environments in the Rocky Mountains (e.g., Birkeland et al., 1987).

Developing soil chronosequences in alpine and subalpine environments is complicated by the overall young age of soils (e.g., Birkeland et al., 1987), which have typically only begun forming in the last 15 cal. kyr BP, since glacial retreat. In fact, few existing alpine chronosequences have attempted to discern variability in soil development at sufficiently short time scales to differentiate post-LGM deposits. The lack of established chronosequences is likely because it is not clear if traditional indicators of soil age such as color change and the presence of illuvial clays can be sufficiently differentiated between these relatively young deposits. Additionally, post-LGM climates have been shown to be quite variable (e.g., Jiménez-Moreno et al., 2008; Johnson et al., 2013), which further complicates chronosequence development.

* Corresponding author.
E-mail address: brjohnson@davidson.edu (B.G. Johnson).

http://dx.doi.org/10.1016/j.catena.2014.12.026
0341-8162/

Post-LGM chronosequences are also complicated if soils are examined across multiple parent materials with different textural characteristics (e.g., sediment size and sorting). Soil chronosequences are typically developed for an individual sequence of landforms including ground moraines (Egli et al., 2001a, 2001b, 2003a), moraines (Berry, 1987; Birkeland and Burke, 1988; Douglass and Mickelson, 2007; Egli et al., 2003b; Mellor, 1986; Taylor and Blum, 1995), loess (Birkeland, 1984b), fluvial terraces (Bain et al., 1993; Engel et al., 1996; Eppes et al., 2008; Layzell et al., 2012a; Leigh, 1996, e.g., McFadden and Weldon, 1987; Shaw et al., 2003), alluvial fans (e.g., McFadden et al., 1989; Mills and Allison, 1995; Ritter et al., 1993) and colluvial deposits (Pollack et al., 2000). In alpine and subalpine areas, however, moraines, alluvial fans, colluvium and valley bottom terraces are found in close proximity to one another and are closely related in terms of form and process (i.e., fans typically grade to terraces). Therefore, if certain soil–age relationships are observable in a small region across multiple landforms and deposits then questions regarding geomorphic relationships can be addressed. For example, alluvial fan and terrace chronologies can be compared in order to identify the source and timing of sedimentation. Such information could also compliment ongoing work in Critical Zone Observatories (e.g., Anderson et al., 2011; Leopold et al., 2011) and inform discussion about soil production (Anderson et al., 2011; Dethier and Lazarus, 2006; Riggins et al., 2011).

This study aims to examine age-dependent soil properties across a variety of post-glacial deposits and landforms in a major, subalpine to alpine drainage basin of the southern Rocky Mountains, USA. Developing this cross-landform chronosequence will provide insights into key pedogenic processes and thresholds acting in these relatively understudied environments. Although this approach challenges fundamental chronosequence assumptions, our data shows statistically significant trends between key soil properties and age despite variation in parent materials, climate and vegetation histories. Additionally, the creation of a multiple-landform relative dating tool for alpine areas will provide geomorphic researchers with a method for better understanding aggradational histories and landscape-scale processes in high elevation environments where datable material is scarce.

2. Study area

2.1. Geography

The Conejos River Valley is located in the southeastern San Juan Mountains in the southern Rocky Mountains (Fig. 1). The Conejos River has four distinct reaches: glaciated headwaters, a glaciated trunk valley, an unglaciated trunk valley, and an alluvial plain where the river flows into the San Luis Valley. The river flows north from its headwaters in the center of the range before flowing east out into the Rio Grande, draining approximately 2300 km^2. The study area for the chronosequence described herein comprises the upper portion of the glaciated Conejos River valley (~35 km in length) plus 6 glaciated tributaries (Rito Azul, North Fork, Middle Fork, Adams Fork, South Fork, and Lake Fork; Fig. 1). Platoro Reservoir (3050 m elevation), which was built in 1951, approximately divides the study area in half. Throughout the field area, the main Conejos River and its tributaries can be further divided into separate sub-reaches. Each sub-reach is characterized by a broad glacial valley, with widths ranging from 300 to 1000 m, separated by steeper canyon reaches, approximately 5 km long, where valley widths range from 50 to 100 m. This pattern of alternating steep and shallow reaches resembles a series of cyclopean steps (Johnson et al., 2010).

During the LGM, the Conejos River basin was covered by the southern extent of the San Juan ice cap, which glaciated all but the highest peaks in the upper Conejos River Valley (Atwood and Mather, 1932). Large valley glaciers extended more than 40 km from the center of the ice cap carving out large U-shaped valleys. In the eastern San Juan Mountains, the glaciers carved deeply into soft volcanic bedrock leaving a high relief landscape where peaks rise to nearly 4000 m and valley floors lie as much as 1000 m below. The volcanic bedrock formed at ~30 ma and is thought to be associated with the end of the Laramide orogeny (Lipman et al., 1970; Lipman, 1974). The eastern San Juan Mountains appear to have been tectonically inactive since the main period of Rio Grande Rift extension ended between 10 and 5 ma (Morgan et al., 1986).

2.2. Climate

Climate in the San Juan Mountains is typical of alpine and subalpine microclimates in the Southern Rocky Mountains and is also strongly influenced by the North American Monsoon (Adams and Comrie, 1997) and El Niño Southern Oscillation (ENSO) cycles. Precipitation in the area also originates from mid-continental troughs and the subtropical jet stream. A nearby SNOTEL station monitors modern climate at roughly the mean elevation of the field area (although not in the field area) where annual temperature is ~1 °C while average annual precipitation is ~75 cm (2/3 of which is winter; 60 cm of snow cover through winter months is typical). Most moisture falls either during the winter months or during the North American Monsoon, which runs from mid-July through August. Maximum river discharge occurs in the late spring (May and June) as temperatures warm and snowpack melts. Since these climate records are recorded at an elevation similar to the middle of the field area, the actual conditions are probably slightly cooler and wetter throughout the upper portion of the valley and warmer and drier throughout the lower portion of the field area. Vegetation varies with altitude but is typically coniferous forest (*Picea engelmannii* and *Abies lasiocarpa*) in the lower field area and alpine tundra in the upper field area (Johnson et al., 2013). Throughout the field area, areas of open grass exist, regardless of elevation, and these were used for soil profile examine to control for differences in vegetation.

Climate is known to have changed in the San Juan Mountains since the LGM (Ariztegui et al., 2007; Carrara and Andrews, 1976; Carrara et al., 1984, 1991; Fall, 1997; Guido et al., 2007; Jiménez-Moreno et al., 2008; Johnson et al., 2013). In particular, there are two paleoclimate records derived from bog cores sampled within 25 km of the field area (Johnson et al., 2013) and within the field area (Deal, 2014). These records provide relatively high-resolution, corroborating, post-LGM records of climate for the field area. Both records provide evidence that cold LGM temperatures lasted until about 16 cal. kyr BP followed by warming until 14–13 cal. kyr BP. A cold Younger Dryas is well-evidenced in both records as is a cold period around 8200 +/− 400. The remainder of the first half of the Holocene was relatively warm and stable. The second half of the Holocene was generally colder with increasing climate switching frequency after 5 cal. kyr BP and again after 3 cal. kyr BP. Records conflict as whether climate was dominantly warm or cold during the latter half of the Holocene (Johnson et al., 2013).

2.3. Quaternary geology

The landforms and deposits of the upper portions of the Conejos River Valley have been mapped at a 1:24,000 scale (Johnson et al., 2010; Layzell, 2010; Layzell et al., 2012b). The most prominent geomorphic features and deposits found within the study area are glacial till, alluvial fans, stream terraces, and colluvium. The expression of landforms and deposits varies in the field area above and below the bedrock constriction that now constitutes the dam for Platoro Reservoir, however the general stratigraphy found in the field area can be correlated (Fig. 2). LGM terminal moraines mapped by Atwood and Mather (1932) lie outside the study area, but are discussed as they provide valuable comparisons for the younger soils in the field area.

Our calculations, based on the timing of deglaciation in the western San Juan Mountains (Guido et al., 2007), indicate that glaciers likely retreated through the field area between 12 and 14 cal. kyr BP. This

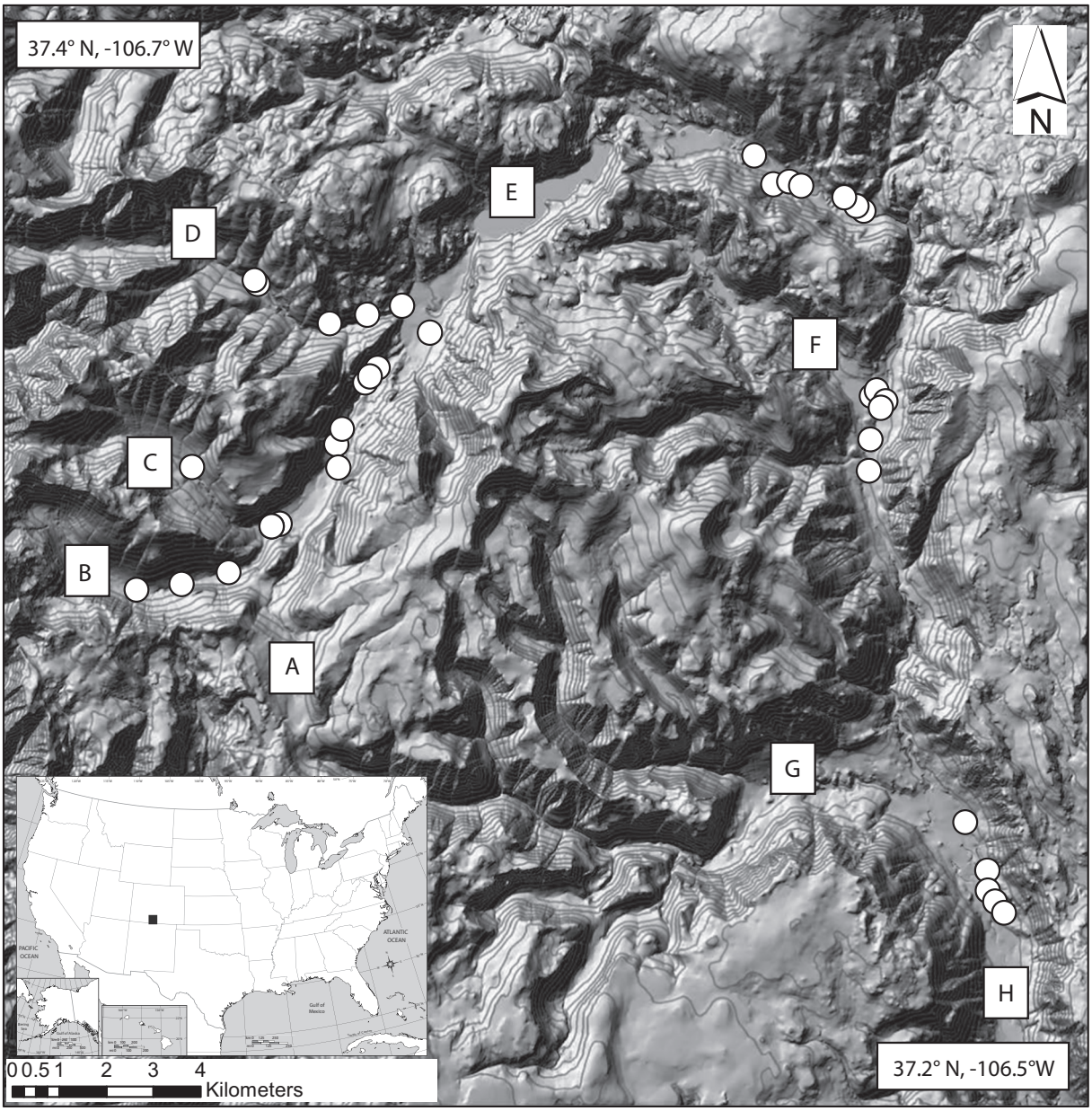

Fig. 1. Map of the field area showing the entire upper Conejos River Valley and tributaries. Circles identify the locations of soil pits. Main features of the drainage include (A) Rito Azul tributary, (B) Middle Fork tributary, (C) North Fork tributary, (D) Adams Fork tributary, (E) Platoro Reservoir, (F) Lake Fork tributary, (G) South Fork tributary, and (H) main upper Conejos River. Contour interval is 50 m.

timing is supported locally by a 12.4 cal. kyr BP basal date from a sediment core taken on an outwash terrace the Conejos River Valley bottom (Deal, 2014). The retreat of glaciers between 12 and 14 cal. kyr BP deposited thick sequences of till in the lower field area and a thin layer of till over the glacially eroded bedrock in the upper field area (Johnson et al., 2010). A large outwash terrace (11–12 cal. kyr BP) and associated alluvial fans formed during the paraglacial period following glaciation, likely as a result of large scale erosion of unvegetated hillslopes. Valley bottom aggradation appears to have continued through 7.6 cal. kyr BP (Layzell et al., 2012b) although the majority of lower elevation hillslopes appear to have stabilized at 9.5 cal. kyr BP (Johnson et al., 2013). Between 9.5 and 11 cal. kyr BP, incision occurred in both areas and was characterized by vertical cutting into the outwash terrace in the lower field area and the stripping of the outwash terrace and till down to bedrock in the upper field area. Aggradation of alluvial fans and terraces continued in the lower part of the field area between 7.6 and 9 cal. kyr BP centered around the 8200 year cold event (Layzell et al., 2012b) which is recognized in paleoclimate records from nearby bogs (Deal, 2014; Johnson et al., 2013). Headwater fans and terraces do not show signs of aggradation during this period (Johnson et al., 2011). Warm stable climate between 7.6 and 6 cal. kyr BP (Johnson et al., 2013) led to incision in both areas, which is shown by an inset terrace that formed between 5 and 6 cal. kyr BP (Johnson et al., 2011; Layzell et al., 2012b). The generally more variable climate between 3.5 and 5 cal. kyr BP (Johnson et al., 2011) led to vertical incision in both areas while increasingly variable climate between 2.5 and 3.5 cal. kyr BP led to lateral incision in the lower field area. After 2.5 cal. kyr BP, a series of fill terraces and alluvial fans dated to between 1 and 2.2 cal. kyr BP indicate an additional period of aggradation.

2.4. Bedrock

The bedrock of the Conejos River Valley is typically composed of volcaniclastic facies, which consist of reworked bedded conglomerates,

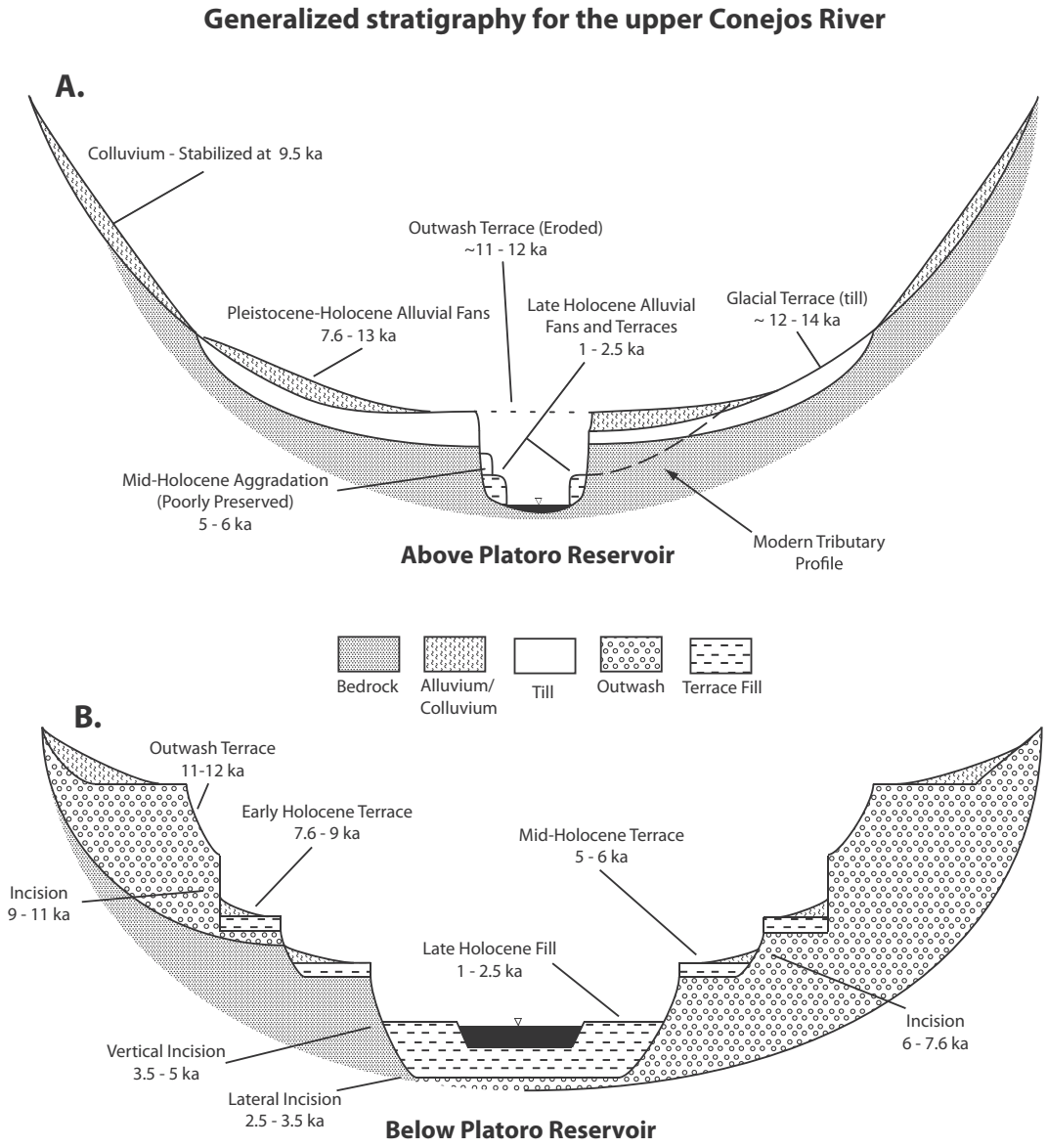

Fig. 2. Generalized stratigraphy of the field area above and below Platoro Reservoir. The diagram highlights both the more subtle stratigraphy above the reservoir and the higher level of map unit preservation below the reservoir.

sandstones and mudflow breccias, as well as aphanitic to porphyritic andesite and rhyodacite (Lipman, 1974, 1975a). These units are locally overlain by volcanic breccias with high dips interpreted to be remnants of a volcanic cone (Lipman, 1975a). The vent facies, which is the dominant bedrock type in the lower valley, is a cliff forming unit which varies in mineralogy laterally but remains erosion resistant throughout the field area. The volcaniclastic conglomerate, which is characteristic of the valley walls and all upper valleys, generally comprises large clasts suspended in a poorly welded ash matrix although the matrix is locally strongly welded and the unit is extremely variable laterally. The conglomerate can resemble the local glacial till as both can consist of large clasts in a soft, ashy matrix.

3. Methodology

A total of 39 soil exposures, ranging from ~19 cal. kyr BP to modern, were excavated and described according to Schoeneberger et al. (2002) and Birkeland (1999) on nine different map units (Table 1) in the field area. Soil pit locations were chosen to minimize variability in vegetation and relief. Thus, on each landform open, flat grassy areas were selected. Observations included descriptions of geomorphic surfaces, horizon thickness and boundaries, color, structure, gravel content, consistence, roots and pores, texture, clay films, as well as standard sedimentary descriptions. Each soil profile was sampled by horizon. Multiple samples were collected where horizons were greater than ~20 cm in thickness. All samples were sieved and the <2 mm fraction analyzed for particle size (pipette method and/or Sedigraph). Organic content was determined using loss on ignition (LOI) and pH was measured on 5 g of soil in 50 mL of distilled water using a handheld probe. Horizon and profile development indices were calculated for different soil properties based on Harden (1982). Profile thickness was identified as the bottom of the BC horizon although depth varied significantly since pits were hand dug in rocky terrain.

The most developed illuvial horizon (B or AB when no B was present) from each pit was selected for Fe extraction based on color, structure, and texture. Fe was extracted from soil samples using both the oxalate (Fe_o) treatment method as well as the dithionite–citrate (Fe_d) treatment (Birkeland, 1999; Mehra and Jackson, 1960). Fe was calculated in ppm and then converted to percent. The oxalate treatment generally removes ferrihydrite (sometimes referred to as amorphous Fe)

Table 1
Unit names and chronology.

Unit	Age range (ka)	Age used in chronosequence (ka)[a]	Dating mechanism
Floodplain	Modern	0	Active geomorphic surface
Late Holocene fluvial terrace	1–2.5	1.38	Radiocarbon dates (Johnson et al., 2011)
Middle Holocene fluvial terrace	5–6	5.41	Radiocarbon dates (Layzell et al., 2012a)
Early Holocene fluvial terrace	7.6–9	8.96	Radiocarbon dates (Layzell et al., 2012a)
Outwash terrace	~11–12	11.5	Stratigraphic relationships
Late Holocene alluvial fans	1–2.5	2.14	Radiocarbon dates (Johnson et al., 2011)
Mid Holocene alluvial fans	5.38	5.38	Radiocarbon date (Johnson et al., 2011)
Early Holocene alluvial fans	7.64	7.64	Radiocarbon date (Johnson et al., 2011)
Pleistocene–Holocene alluvial fans	7.6–13	10.3	Radiocarbon dates for Holocene limiting age (Johnson et al., 2011) and stratigraphic relationships
Colluvium	9.5–9.9	9.7	Radiocarbon dates (Johnson et al., 2011)
Glacial till	~12–14	13	Stratigraphic relationships and retreat timing from Guido et al. (2007) and Deal (2014)
Last Glacial maximum recessional moraines	~19	19	Inferred from Guido et al. (2007)

[a] Ages for ^{14}C dated units are average calibrated ^{14}C ages (ka) rounded to nearest ten. All other ages are the midpoint of the inferred age range.

from soils. Ferrihydrite is mainly a product of in situ weathering of parent material within the profile, although some also comes bound in organics, and forms as a coating on parent material either via precipitation from water or bacterial fixation (Fortin and Langley, 2005). Ferrihydrite is metastable and will crystallize into goethite and then hematite over time (Schwertmann et al., 1999). A dithionite–citrate treatment will remove goethite and hematite as well as ferrihydrite and thus a ratio of Fe_o/Fe_d provides a measure of crystallization and oxidation with numbers closer to zero being more crystallized/oxidized (Birkeland, 1999; McFadden and Weldon, 1987). Birkeland (1984a) suggested that extraction procedures are less than precise in terms of removing known Fe forms. As a consequence, extractable Fe data will be discussed in terms of method and not necessarily the mineral species. Select Fe samples were run a second time to determine the error inherent in the method. All duplicated samples were within 6% of the original value with the average being 4%. Changes in pedogenic Fe are reflected in the Fe activity ratio (Fe_o/Fe_d). This ratio negates the difference in the initial Fe_o content of the parent material and emphasizes the formation of Fe oxides due to weathering processes.

Chronological control is provided by radiocarbon (^{14}C) ages determined by the University of Georgia Center for Applied Isotope Studies using an accelerator mass spectrometer (AMS). Map units are dated by 12 ^{14}C dates from charcoal preserved in various surficial deposits (Johnson et al., 2010; Layzell et al., 2012b, Table 1). All samples for radiocarbon (^{14}C) were taken from walls of soil exposures and were taken from more than 30 cm depth to avoid the effects of bioturbation. Stratigraphic relationships between landforms were used to determine the approximate age of landforms adjacent to dated landforms. All dates are calibrated.

4. Results and discussion

4.1. Overview

The soils examined in this study have formed over the last 19 cal. kyr BP with most being younger than 13 cal. kyr BP. The age of these soils is very young in comparison to many other published chronosequences (Berry, 1987; Engel et al., 1996; McFadden and Hendricks, 1985; McFadden and Weldon, 1987; Taylor and Blum, 1995; Tsai et al., 2007). Thus, it is not surprising that differences between the oldest soils in the area and the youngest soils in the area are not profound. For instance, soils in the area often do not exhibit sufficient levels of development to effectively utilize traditional indicators of soil age such as color change. Nevertheless, certain soil properties were found to evolve progressively through time. As would be predicted, these trends become clearer when other soil forming factors (i.e. parent material) are accounted for.

Generally, studies would attempt to minimize variations in parent material and geomorphic history (Birkeland et al., 2003) when creating a chronosequence. Our focus on the evolution of the entire Conejos River Valley landscape, as opposed to just the evolution of particular landforms, means that soils have intentionally been analyzed on a variety of geomorphic surfaces. While this is advantageous in studying landscapes, it adds complexity to the chronosequence. Variations in parent material add variance to chronofunctions as initial differences in texture, permeability, chemistry, and porosity influence the development of soils through time. Here we discuss the evolution of soils on individual parent materials with the ultimate goal of identifying soil properties that are good indicators of age across multiple landforms and deposits.

4.2. Glacial deposits

Glacial sediments make up the two oldest deposits examined. The crests of downstream recessional moraines (~19 cal. kyr BP) were predominantly loam with variable sand content and highly developed horizonation (A/AB/Bw/BC/C) and relatively deep profile thicknesses (>1 m; see Appendix A). Clay percent profiles display illuvial peaks in the AB and B horizons (Fig. 3) with decreasing clay with depth indicating little clay content in the original glacial deposits. Extractable Fe ratios from the moraines are relatively low, ranging from 0.17 to 0.26 (Table 2). Younger, undifferentiated till within the field area (~12–14 cal. kyr BP) displays similar horizonation (A/AB/Bw/C; see Fig. 4 for examples of profiles) with slightly thinner profile thicknesses (75–90 cm; Appendix A). Slight clay content peaks occur in AB horizons indicating some illuvial deposition of clays (Fig. 3). Extractable Fe ratios are relatively low but exhibit a wide range (0.3–0.63; Table 2).

Soils developed in glacial till have well-defined B horizons, however, the soils display significant variation in extractable Fe content, soil color, and overall horizonation. It is therefore likely that the rate of soil development through time has been influenced by the intrinsic variability of glacial sediment (e.g., Evans and Benn, 2004). For instance, local initial differences in clay content may influence the hydrology of the soil and influence its weathering rate by altering the rate at which the soil absorbs water. Weathered depth is fairly consistent (76–86 cm) between sites although this depth is less than younger soils in the area, and may reflect erosion of moraine crests as has been observed elsewhere (Birkeland and Burke, 1988). Overall, the sedimentology of observed glacial deposits varies significantly as does their post-retreat geomorphic modification.

In previous studies, soils in glacial material examined over multiple glaciations show strong age-dependent trends (Berry, 1987), however soils in post-LGM recessional glacial deposits show a much more subtle variation through time. Furthermore, glacial deposits in the field are time-transgressive and soils on till are not all the same age. The

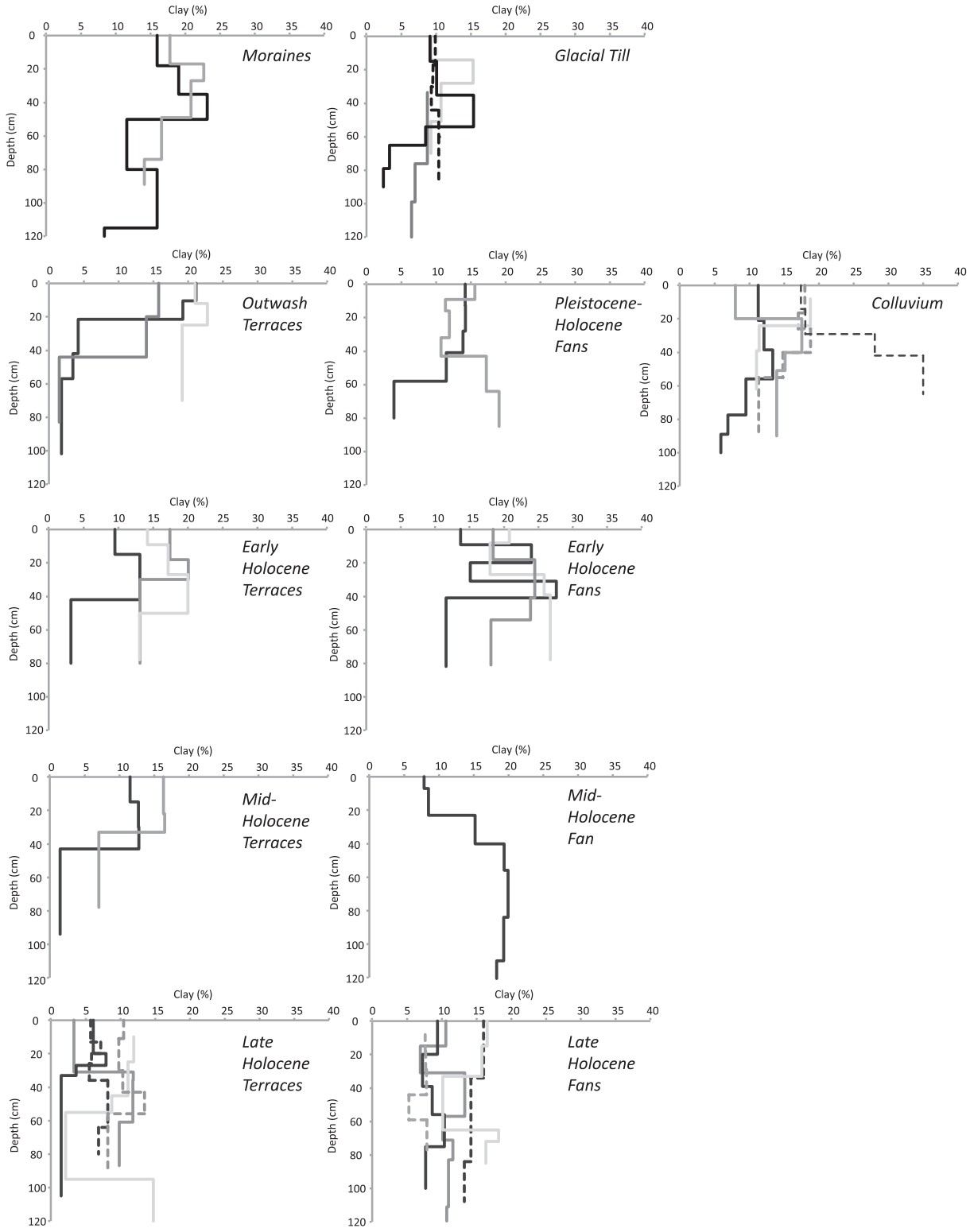

Fig. 3. Clay profiles for soil profiles by landform with each line representing a unique profile. Weak trends indicate that clay content generally increases with time. However, significant differences exist between landform types and individual profiles.

maximum (19.5 cal. kyr BP) and deglaciated (12.3 cal. kyr BP) ages provided by Guido et al. (2007) provide a retreat rate of 7.8 km/ky, which is similar to rates observed in other regions (Gosse et al., 1995). This retreat rate indicates that deglaciation would have reached the lower extent of the field area as early as 18 cal. kyr BP while deglaciation would not have reached the reservoir until 15 cal. kyr BP, and the headwaters until much more recently.

4.3. Alluvial fans

The oldest alluvial fans in the area began forming during the Late Pleistocene but aggradation continued into the early Holocene (as late as 7.6 cal. kyr BP; Johnson et al., 2010). Deposition was discontinued in the early Holocene as their source channels have incised into the fan surface. The cumulic (i.e. slow accumulation of sediment coincident

Table 2
Soil pit chronofunction data.

Parent material	Location	Unit	Age (ka)	B horizon clay %	Max horizon structure	pH	Fe_o/Fe_d
Fluvial	Platoro	Floodplain	0	No B horizon	0.42	6.08	0.71
	Lake Fork	Floodplain	0	No B horizon	0.46	5.53	0.8
	South Fork	Floodplain	0	No B horizon	0.46	5.44	0.73
	Platoro	Late Holocene terrace	1.38	11.1	0.46	5.31	0.62
	Lake Fork	Late Holocene terrace	1.38	13.5	0.58	5.69	0.57
	South Fork	Late Holocene terrace	1.38	8.0	0.46	6.27	0.67
	Three forks	Late Holocene terrace	1.38	8.2	0.75	5.06	0.66
	Three forks	Late Holocene terrace	1.38	9.8	0.75	5.00	0.57
	Middle fork	Late Holocene terrace	1.38	11.1	0.88	4.56	0.57
	Platoro	Mid Holocene terrace	5.41	12.8	0.50	5.86	0.59
	Lake Fork	Mid Holocene terrace	5.41	16.5	0.63	5.52	0.52
	Platoro	Early Holocene terrace	8.96	13.1	0.46	5.12	0.44
	Lake Fork	Early Holocene terrace	8.96	20.1	0.75	5.67	0.42
	South Fork	Early Holocene terrace	8.96	20.0	0.75	5.91	0.39
	Platoro	Outwash terrace	11.5	15.8	0.46	5.49	0.41
	Lake Fork	Outwash terrace	11.5	22.8	0.75	5.45	0.41
	Adams Fork	Outwash terrace	11.5	20.0	0.63	4.70	0.39
Alluvial fans	Platoro	Late Holocene fan	2.14	14.2	0.50	5.14	0.18
	South Fork	Late Holocene fan	2.14	15.8	0.67	6.28	0.72
	Middle Fork	Late Holocene fan	2.14	7.6	0.44	4.70	0.60
	Upper Trunk Valley	Late Holocene fan	2.14	8.6	1.00	5.19	0.91
	Upper Trunk Valley	Late Holocene fan	2.14	13.3	0.75	5.53	0.70
	Upper Trunk Valley	Mid Holocene fan	5.38	19.9	0.75	5.02	0.54
	Platoro	Early Holocene fan	7.64	24.0	1.00	5.65	0.91
	Lake Fork	Early Holocene Fan	7.64	18.0	1.00	5.96	0.33
	South Fork	Early Holocene fan	7.64	24.5	1.00	6.27	0.13
	Upper Trunk Valley	Pleistocene–Holocene fan	10.3	14.2	0.75	4.79	0.46
	Upper Trunk Valley	Pleistocene–Holocene fan	10.3	19.1	0.75	4.96	0.53
Colluvium	Adams Fork	Coluvium	9.7	13.4	0.75	5.44	0.35
	Adams Fork	Coluvium	9.7	18.8	0.75	5.72	0.48
	Upper Trunk Valley	Coluvium	9.7	18.7	0.75	5.53	0.39
	Platoro	Coluvium	9.7	17.6	0.50	5.69	0.46
	South Fork	Coluvium	9.7	35.0	1.00	5.91	0.38
Glacial	Adams Fork	Glacial till	13.0	7.0	0.69	5.08	0.48
	Upper Trunk Valley	Glacial till	13.0	15.3	0.63	5.22	0.63
	North Fork	Glacial till	13.0	15.4	0.75	4.94	0.30
	Middle Fork	Glacial till	13.0	10.4	0.75	4.90	0.52
	Terrace Reservoir	Glacial moraine	19.0	23.2	0.75	6.06	0.26
	Cumbres Bog	Glacial moraine	19.0	22.7	0.75	5.06	0.17

with weathering) nature of these Pleistocene–Holocene soils leads to varied horizonation including buried soils, deep profile thickness (1–2 m), and highly variable clay-depth profiles (Appendix A, Fig. 3). Extractable Fe ratios range between 0.46 and 0.53 (Table 2). Late Holocene alluvial fan (1–2.5 cal. kyr BP) soils are also cumulic and are characterized by highly variable horizonation (A/ABw/Bw/C to Aw/Bw/Bb/C), profile thickness (25 to >130 cm) and clay content (Appendix A, Fig. 3). It is worth noting that while the soil profiles are cumulic and contain buried horizons, the surface of the fans does not appear to be active based on the incision of modern streams. Extractable Fe ratios are highly variable, ranging from 0.18 to 0.91 (Table 2).

It is difficult to differentiate the two generations of Holocene alluvial fans (5–6 cal. kyr BP and 1–2.5 cal. kyr BP) in the field based upon their morphological expression alone. Nevertheless, soil development, along with stratigraphic relationships (when they are observable), is useful in identifying the age of these features. The presence of buried soils in Holocene alluvial fans complicates the comparison of the properties of the surface soils of these profiles (see below). Buried soils can be difficult to identify in the field for these young deposits because they are poorly developed at the time of burial, and the burial deposit is often shallow, resulting in soil development that overprints the underlying buried horizons. Peaks in organic content at depth in these deposits, however, are similar to those that have been used for identifying buried soils in other studies (McDonald and Busacca, 1990) and allow us to identify numerous buried soils in alluvial fan deposits The extremely weak development of many of the surface soils of fan deposits (A/C horizonation) provides evidence that fan sedimentation or reworking likely continued in some locations through the late Holocene, even on alluvial fans for which the majority of the deposit, as indicated by buried soils, is significantly older.

4.4. Fluvial sediments

Fluvial sediments make up the largest number of individual landforms in the field area. The soils on the oldest fluvial deposits (outwash terrace, 11–12 cal. kyr BP) are typically silty loams and have relatively well developed horizonation (A/AB/Bw/BC), profile thicknesses of ~1 m, and low Fe ratios (0.39–0.41) (Appendix A). The upper horizons contain some clay but clay content generally decreases with depth from A to B horizons (Fig. 3). The Early Holocene fluvial terraces (7.6–9.0 cal. kyr BP) have slightly less mature horizonation (A/Bw/2BC/2C) and moderate profile thickness (~80 cm) (Appendix A). Some illuvial clay is present in B horizons and extractable Fe ratios are generally low (0.39–0.59) (Table 2). Mid-Holocene fluvial terrace soils (5–6 cal. kyr BP) are moderately developed as shown in horizonation (A/Bw/2C), Fe ratios, and profile thickness (78–94 cm) (Appendix A) Clay content is fairly consistent between the A and B horizons (Fig. 3). Late Holocene fluvial terrace soils appear less developed which is consistent with their approximate age (1–2.5 cal. kyr BP). Profile thicknesses are typically thinner (37–87 cm) despite the common occurrence of buried horizons (Appendix A) and there is no consistent pattern of clay content with depth (Fig. 3). Extractable Fe ratios for soils on late Holocene fluvial terraces are generally higher than those on other terraces but have a broad range (0.6–0.91; Table 2).

Fluvial deposits display the clearest evolution of soil properties through time. Pedogenic clay content and extractable Fe ratios, which produce statistically significant but weak trends with age across all

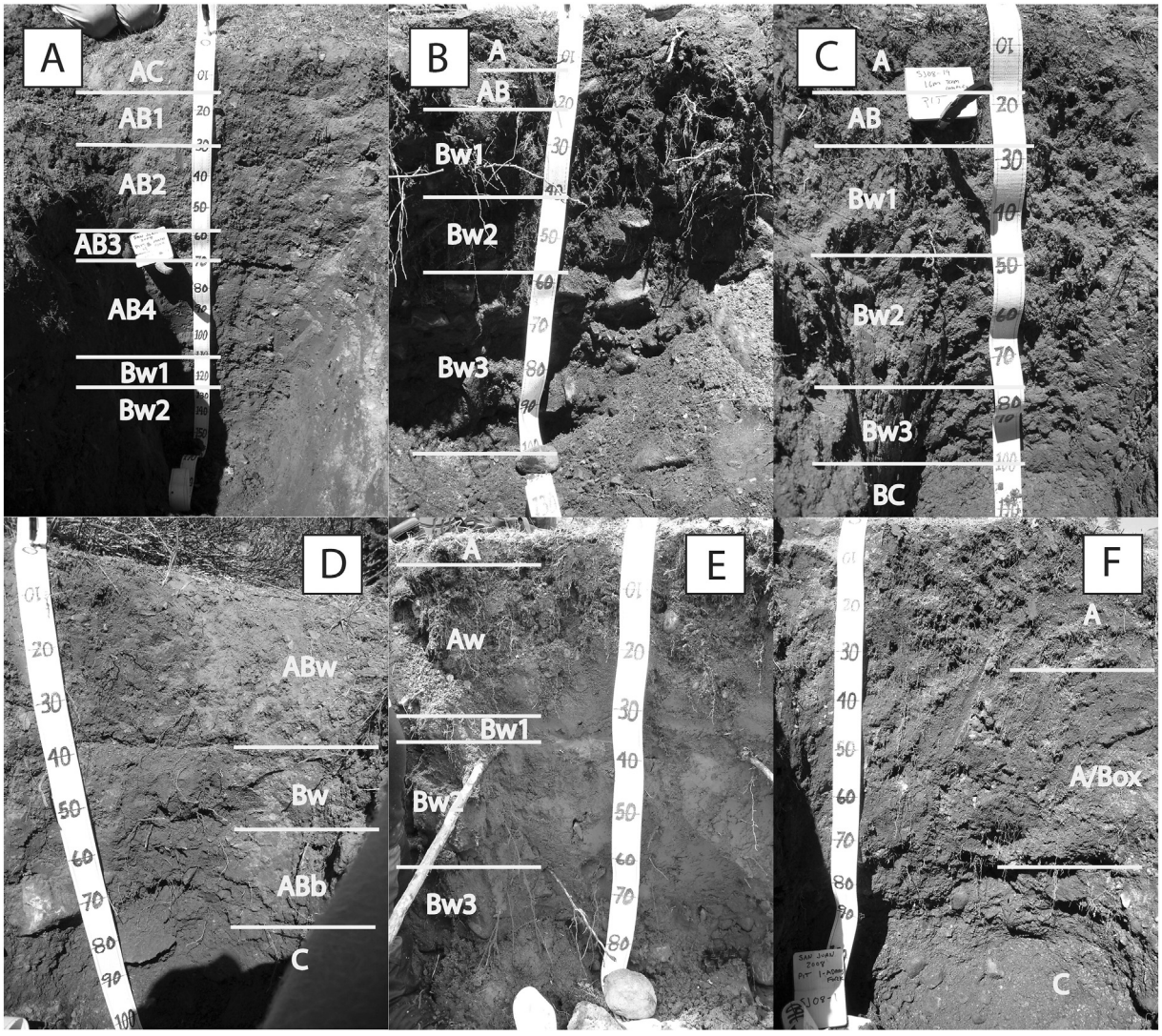

Fig. 4. Example soil pit photographs. Sample profiles show the small differences in soil development between soils of different ages. Profiles include (A) Pleistocene–Holocene alluvial fan, (B) outwash terrace, (C) terminal moraine, (D) Late Holocene alluvial fan, (E) Late Holocene terrace, and (F) glacial terrace. See Table 2 for ages.

deposits ($R^2 = 0.23$ and 0.38, respectively) have much stronger trends with age in fluvial sediments alone ($R^2 = 0.71$ and 0.84, respectively; Figs. 5 and 7). The difference in the degree of correlation between all soils and soils developed in alluvium alone highlights the difficulties in creating a chronosequence across multiple landforms and deposits. Soil property–age trends are most clear in terrace (fluvial) soils and reflect the uniformity of the deposit's sedimentology. Also, terrace surfaces, once abandoned, are inherently more stable than the sloping surfaces of alluvial fans, colluvium, and glacial deposits. As such, the soil forming factors affecting fluvial terraces through time are more consistent between terrace surfaces of differing age as has been demonstrated by a large number of chronosequences in a wide variety of locations (e.g., Eppes et al., 2008; Leigh, 1996; McFadden and Weldon, 1987).

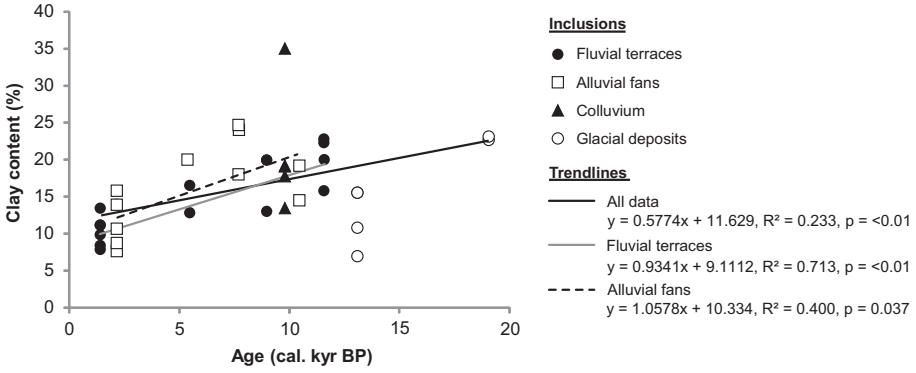

Fig. 5. Soil chronofunctions developed using maximum B horizon clay content. The relationship between B horizon clay content and time is weak but statistically significant. This relationship becomes significantly stronger when only terraces are examined.

Clay profiles from terrace soils show some weak trends through time (Fig. 3). In the oldest fluvial deposits (11–12 cal. kyr BP), clay content generally decreases with depth. We interpret this trend to indicate that the major source of clay is eolian dust. Although unweathered C horizons were not encountered in most locations, where they were, they were typically loamy sands. Early Holocene fluvial terraces (7.6–9 cal. kyr BP) display peaks in clay in the B horizons indicating illuvial accumulation in the soil profile. Mid-Holocene terraces are characterized by decreasing clay content with depth, suggesting that not enough time has passed for illuvial clays to have accumulated. Clay profiles in young Holocene terraces (1–2.5 cal. kyr BP) are extremely variable, which is likely the result of initial differences in sedimentology and not pedogenic processes.

Terrace soils commonly have clay and silt peaks near or at the surface indicating significant inputs into soil profiles through eolian influx. Since all soils display eolian material at the surface, the silt peak in the fluvial sediments is likely due to the fact that little initial sedimentary silt is in the original fluvial sand and gravel deposits. Dust inputs are supported in our data by 1) similarities in A horizon properties from all soils, 2) a lack of gravel in the top 2 cm of most soil profiles even when the parent material is gravel rich, 3) a low degree of correlation between Fe_d and clay content which has been shown to reflect dust additions (McFadden and Hendricks, 1985), and 4) research with similar conclusions in the Rocky Mountains (e.g., Birkeland et al., 1987).

4.5. Colluvial deposits

Colluvial deposits (~9.5 cal. kyr BP) are mantled by soils that are characterized by A/AB/B–Bt–C horizonation and deep weathering profile thicknesses (85–120 cm; Appendix A) indicating that these soils are more developed than most others in the field area. Illuvial clays are present in most B horizons and are characterized by up to 35% content, occasional clay films, and clay peaks in the B horizons (Appendix A and Table 2, Fig. 3). Extractable Fe ratios are relatively low (0.35–0.48; Table 2).

Colluvium on lower hillslopes in the upper Conejos River Valley appears to be stable and has been dated to 9837 +/− 72 and 9567 +/− 67 calibrated years (Johnson et al., 2010). The fact that evidence for illuviation (e.g., Bt horizons and clay films) were only observed in deposits dated to ~10 cal. kyr BP or older (Appendix A) may indicate that this may be the amount of time required for illuvial clays to accumulate in B horizons. However, not all Pleistocene–Holocene and older soils show evidence of illuvial clays (Appendix A), likely due to differences in initial sedimentology or eolian dust inputs.

4.6. Bedrock variability

Bedrock variability in the field area likely influences the development of soils in various deposits. Since all soils examined are formed in sediment, the upstream/upslope bedrock characteristics will be reflected in that sediment and thus in the pedogenesis of the deposits. This influence is probably minimized along the main trunk valley where sediment mixing through the fluvial system is more thorough. Such mixing likely aids the strong age–soil development trends that we observe in those deposits. In contrast, the overall higher variability that we observe in alluvial fan soil properties may be attributable, in part, to the variability in the underlying bedrock of source areas for different fans. For instance, an individual alluvial fan has a single source area. Thus, it may be more difficult to compare fans to each other because initial differences in grain size and iron mineralogy may differ significantly. Therefore, it would be useful to identify any direct correlations between pedological characteristics and mapped lithofacies in contributing basins. However, variability within each bedrock map unit likely precludes such simple correlations even if source areas for individual fans could be clearly identified as coming from the same geologic unit.

For example, the most common rock type in the area, the "volcaniclastic facies of the Conejos Formation" (Lipman, 1974, 1975b), varies from a well-welded breccia to an ash-matrix conglomerate resembling glacial till. This facies also contains reworked clasts of unknown origin and variety. The mineralogy, erodibility and sediment size of each of these sub-facies vary greatly which would impact texture and iron mineralogy. Thus, it would require more detailed mapping of bedrock in each sub-basin, as well as an assumption of the proportion of sediment derived from each region of the basin to make such an assessment.

4.7. Soil property chronofunctions

Many soil morphological properties exhibit trends as a function of age in the Conejos River Valley. These trends are observed across multiple landforms, but as would be expected there are stronger soil–age correlations for soils developed in deposits with analogous parent materials and geomorphic histories (e.g. till, fluvial sediment, alluvial fan sediment).

4.7.1. Horizonation

Soils developed throughout the field area show increased horizonation morphology with age. For example, the recessional moraines outside the field area are the oldest and have the thickest B horizons. Similarly, other older units, including Early Holocene alluvial fans, have better developed B horizons (i.e. Bt horizons) compared to younger fans. The increasing horizonation trend is particularly strong in soil profiles on terrace deposits, which show distinct horizon development with age. Profiles in terraces typically display increased B horizon development from A/AB/C horizonation on the floodplain to A/Bw/2C on younger surfaces (e.g., Late Holocene) to A/Bt/2C on older terraces (e.g., Early Holocene and Pleistocene–Holocene).

A horizon development is similar on all units in the field area. A horizons are typically 8–30 cm thick, with very dark to dark brown colors (10YR 2/2–10YR 4/3), silty loam textures and weak structure. Furthermore, gravel content in A horizons is consistently less than 10% despite the high gravel percentages in the underlying sediment. These relatively uniform A horizons, regardless of deposit parent material or age, speak to the important influence of dust in contributing to soil profile chemistry and sedimentology in this setting. There does not appear to be correlation between dust thickness and age indicating a steady state thickness caused by eluviation of fine material into the underlying gravel rich material. Silt films are common on ped faces in most soil profiles.

4.7.2. Particle size

Clay content in the B horizon shows statistically significant positive trends with time for all examined soils ($R^2 = 0.23$, $p = <0.01$) and these correlations are stronger for individual landform–sediment assemblages such as fluvial terraces ($R^2 = 0.71$, $p = <0.01$) and alluvial fans ($R^2 = 0.40$, $p = 0.037$; Fig. 5). Clay content for terrace units ranges between 8.0 and 13.5% on Late Holocene terrace deposits and between 15.8 and 22.8% on the oldest terrace (outwash) deposits in the study area (Table 2). Clay contents ranged between 7.6 and 15.8% on Late Holocene fan units and between 18.0 and 24.5% on Early Holocene fan units. Clay contents were slightly lower on Pleistocene–Holocene fans ranging from 14.2 to 19.1%. Clay contents of up to 35.0% were documented on colluvial units, but were overall variable. Examining the relationship between clay content and time across all landforms is complicated by the variable clay contents in colluvium and relatively low clay contents in glacial till deposits. The low clay content in glacial till is likely a function of the initial sedimentary characteristics rather than pedogenic processes as unweathered glacial till in the area appears to be silt rich.

4.7.3. Structure

Clay content of the soil is an important factor in the formation of blocky structure (Birkeland, 1999). One might therefore expect to see similar trends over time between structure and clay content. However, results indicate that the trends between quantitative structure indices and time do not have the same strength of correlation or statistical significance as clay–age trends (see Figs. 5 and 6). Structure–age trends do indicate a statistically significant trend (at the 0.1 alpha level) with time when all deposits are considered, however, this correlation explains almost none of the variance ($R^2 = 0.08$, $p = 0.083$, Fig. 6). The documented variability in soil structure is likely due to the fact that given the relatively young age of the soils, subtle changes in structure over time are not readily observable in the field. Aside from clay content, initial differences in sedimentology of all grain sizes would further complication the relationship between structure and time. Specifically, terraces, which typically have the strongest chronofunction correlations through time, are among the weakest correlation here because clast-supported and sand dominated deposits are less susceptible to improving structure through time.

4.7.4. pH

Soil pH typically increases with depth for the studied soils, becoming more alkaline. Whereas many soils will exhibit significant acidification with time, particularly over long time scales (Haugland and Owen, 2005) overall our results indicate no statistically significant trends with time when examining all deposits ($R^2 = 0.01$, $p = 0.591$, Fig. 7) or fluvial deposits alone ($R^2 = 0.01$, $p = 0.679$, Fig. 7). The lack of any good correlations between pH and time are likely attributable to the consistent dust thickness on soil surfaces, which would dampen the overall reduction of pH through time. It may also be that these soils are not old enough to show age trends in pH.

4.7.5. Extractable Fe ratio

Soils developed in Quaternary deposits usually oxidize progressively with time as pedogenic Fe oxides form within the soil. In our field area quantitative differences in color hue that would be attributable to formation of Fe oxides were not differentiable between different deposits of a similar age regardless of landform type. This lack of distinction likely reflects the resolution of the Munsell color system, and not a lack of difference in color. Subtle color differences between deposits of different ages were regularly observed, however, we were unable to quantitatively resolve these differences with the standard soil Munsell chart.

Analysis of extractable Fe content, however, revealed statistically significant trends through time regardless of landform/deposit (Fig. 8). Initial differences in Fe content are highlighted by the fact that neither Fe_o nor Fe_d shows any trends through time. However, Fe_o/Fe_d values range from 0.13 to 0.91 with high values indicating less weathering. Maximum values of Fe_o/Fe_d were typically found on younger deposits (e.g. floodplain and Late Holocene terrace and fan deposits) indicating a relatively low degree of Fe crystallinity (McFadden and Hendricks, 1985). The declining trend in Fe_o/Fe_d is expected (Eppes et al., 2008; Shaw et al., 2003) and is attributed to the conversion of amorphous hydrous oxides (Fe_o) to more stable, crystalline forms (Fe_d) over time.

The Fe ratio trend is strongest when examined exclusively across terrace deposits ($R^2 = 0.84$, $p = <0.01$, Fig. 8) but is also observable across all landforms ($R^2 = 0.38$, $p = <0.01$, Fig. 8) despite differences in parent material and geomorphic history. Even when Fe data for terrace deposits is removed, the trend across all other landforms and deposits remains statistically significant at the 0.05 alpha level ($R^2 = 0.22$, $p = 0.029$). The weaker relationship with time across all deposits is similar to that seen in clay content and illustrates how different parent materials and landform history can complicate an otherwise clear trend. In particular, soils developed in alluvial fans exhibit a wide range of extractable Fe ratios that diminish the strong trend in Fe_o/Fe_d documented from terrace deposits.

4.7.6. Understanding Fe variability on alluvial fans

The wide range of extractable Fe ratios observed in fans may be due to intrinsic controls on fan development. Studies have long shown that the response of fans to extrinsic forcing in a given setting is not always similar and that therefore fan development is often controlled by intrinsic factors that differ between individual drainage basins, particularly at post-glacial time scales (Eppes and McFadden, 2008, e.g., Wells et al., 1987). As previously mentioned, fan soil variability may be attributable in part to different bedrock source areas, however, we are unable to identify any distinct pedological differences in fans sourced from distinct areas. It is important to note that the data used to develop chronofunctions in this study were determined from surface soils. The flashy hydrology typical of small tributaries in this setting likely resulted in fan surfaces that have differing geomorphic histories. In other words, stratigraphically related fan surfaces may not have stabilized at the same time and so surface soils on a given fan unit may actually differ in age. This hypothesis is supported by the fact that removing data for alluvial fans that do not have direct age control produces a statistically significant correlation that explains a much greater proportion of the variance ($R^2 = 0.68$, $p = <0.01$, Fig. 8). However, if surface soils on a given fan unit are different ages then one might expect to see similar variability in terms of fan clay content. As previously noted, clay–age relationships are statistically significant for alluvial fans ($R^2 = 0.40$, $p = 0.037$). Excluding clay content data for alluvial fans that do not have direct age control increases the significance slightly but, in contrast to Fe ratios, explains less of the variance ($R^2 = 0.23$, $p = 0.01$). Another possibility is that the variability documented in Fe ratios for alluvial fans represents an inherited signal. It is possible that fans are reworking older material preserved on lower slopes in individual drainage basins. This would account for the low Fe ratios, which are more typical of glacial deposits, found in some of the late and early Holocene fans.

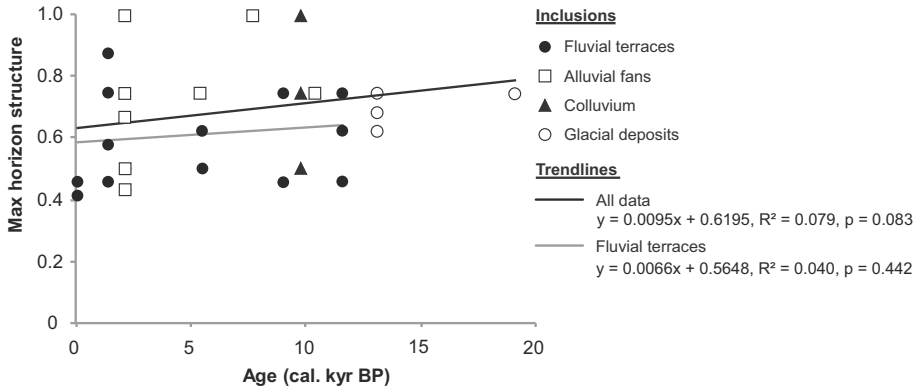

Fig. 6. Soil chronofunctions developed using soil structure indices. There is no discernable relationship between maximum profile structure and time.

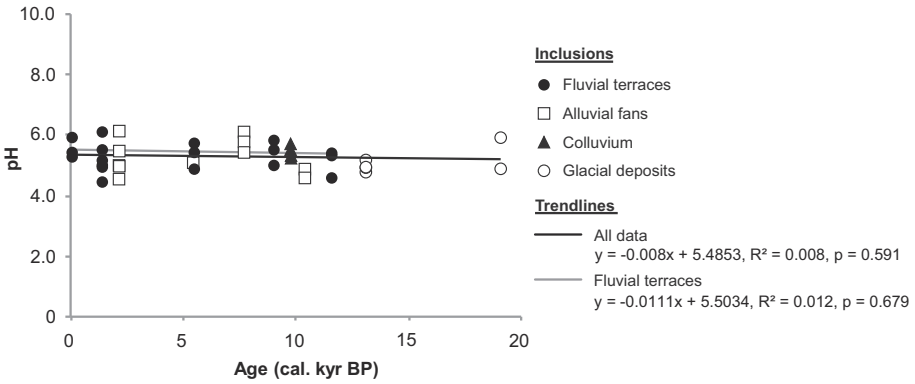

Fig. 7. Soil chronofunctions developed using average profile pH. pH remains relatively constant through time and across parent materials.

5. Conclusions

This study found that certain soil properties revealed trends with time from soils developed in a variety of landforms and deposits in the subalpine to alpine environments of the southern Rocky Mountains. In particular, horizonation, clay content and extractable Fe ratios (Fe_o/Fe_d) presented discernible and statistically significant trends across late-Pleistocene and Holocene time scales. These properties therefore provide a useful tool for correlating these relatively young deposits, assigning ages and interpreting the geomorphic history of these understudied environments.

Overall soil–age trends, as well as soil complexities, that we observe for this relatively young chronosequence are similar to those observed in older soil counterparts across a range of environments (Bain et al., 1993; Berry, 1987; Birkeland and Burke, 1988; Birkeland et al., 1989, e.g., Egli et al., 2001a, 2003b; Engel et al., 1996; McFadden and Weldon, 1987; McFadden et al., 1989; Mellor, 1986; Ritter et al., 1993; Taylor and Blum, 1995). Statistically significant age-related trends in soil development over post-glacial time are preserved in a variety of deposits of the southern Rocky Mountains. As would be expected, age relationships are stronger for soils developed in analogous landforms that were deposited and abandoned synchronously (e.g. terraces). Variability in soil properties throughout a single mapping unit lessens over time as the initial variability in parent material texture is homogenized through soil forming processes. The resolution of measurement of some soil properties such as color and structure preclude drawing quantitative age–soil relationships even when qualitative variability is evident. The common occurrence of cumulic soils in the subalpine landscape of the study area rendered weathered depth ineffective in determining age as some of the youngest soils were also the thickest. The vertical dispersion of accumulating illuvial clays and Fe oxides caused by cumulization also likely accounts for the variability in these measures that we observe in alluvial fan deposits. Taking total horizon content into account rather than percentages may help but remains untested in Fe ratios. Our examination of soils developing in surficial alluvial fan deposits revealed that there is likely sufficient age variability between individual fans within a single mapping unit that certain soil properties are variable between these deposits. We suspect that additional age control would yield a stronger correlation between fan ages and soil development in general. Finally, the likelihood that fans are remobilizing material from lower hillslopes in individual drainage basins would also explain some of the observed variability. In sum, this study of soils forming in the post-glacial landforms and deposits of the southern Rocky Mountains highlights the usefulness of soil-profile-derived data for providing both calibrated-dating as well insight into the post-glacial history of this complex landscape.

Acknowledgments

We would like to thank Josh Link, Jeremy Poplawski, and Ben Rote for their assistance in the field. Suzanne Ching, Mike Murphy, Claire Chadwick, and Jon Watkins all assisted us with samples in the laboratory. USGS EDMAP grants provided funding for mapping over two years: #07HQAG0051 (BGJ, MCE) and #G09AC00131 (TAL, MCE). BGJ also received funding from GSA Student Grant program and from the Colorado Scientific Society. Special thanks to the Chama Institute of Arts and Sciences for logistical support including lodging and food.

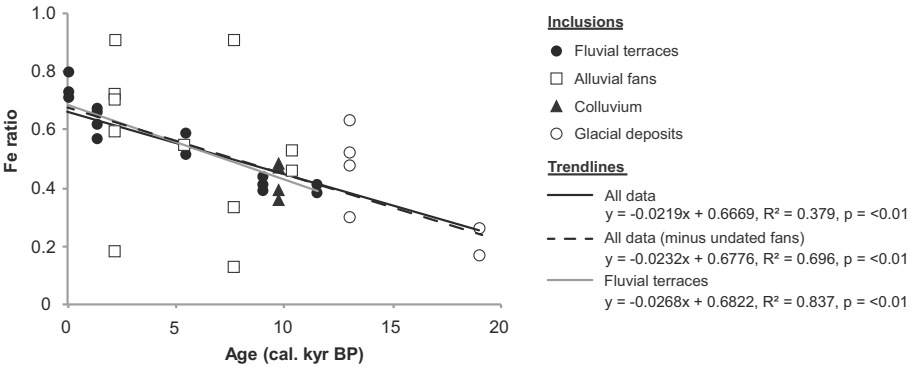

Fig. 8. Soil chronofunctions developed using extractable Fe ratios. Iron activity ratios become significantly lower through time. The trend is strongest among fluvial terraces but can also be seen across parent materials. Alluvial fans appear to the least consistent through time.

Appendix A. Soil field descriptions for all soils

			Depth	Color		Gravel			Consistence		Clay			
Unit	Locality	Horizon	(cm)	Moist	Dry	(%)	Texture	Structure	Wet	Moist	Films	Boundary	Roots	Pores
Flood plain	Platoro	A	0–8	10YR 3/2	10YR 4/3	0	SiL	2 f gr	ss ps	vfr	–	c s	2m 3f 3vf	1f 3vf
		AB	8–38	10YR 3/3	10YR 5/4	<10	LS	2 f gr	ss ps	vfr	–	c s	2m 2f 2vf	2f 3vf
		2C	38–49	10YR 2/2	10YR 5/2	>75	S	sg	so po	lo	–	–	1m 1f 2vf	–
Flood plain	Lake Fork	A	0–10	10YR 2/2	10YR 4/3	<10	SL	2 vf sbk	ss ps	fr	–	a s	1c 1m 2f 3vf	2m 2f 3vf
		AB	10–16	7.5YR 2.5/2	10YR 5/4	<10	SL	s f sbk	ss ps	fr	–	a s	1f 2vf	2fvf
		C	16–21	10YR 2/2	10YR 5/3	25	S	sg	so po	lo	–	a s	3vf	–
		C2	21–27	10YR 3/2	10YR 5/3	<10	LS	sg	so po	lo	–	a s	2f 1vf	–
		2C	27–42	10YR 2/2	10YR 5/3	50–75	LS	sg	so po	lo	–	–	1f 1	–
Flood plain	South Fork	A1	0–8	10YR 3/2	10YR 3/3	0	SL	2 m gr	ss ps	vfr-fr	–	c s	1f 3vf	2f 3vf
		A2	8–24	10YR 3/2	10YR 5/3	0	SL	2 f sbk	ss ps	vfr-fr	–	a s	2f 3vf	1m 1f 3vf
		2C	24–45	10YR 2/2	10YR 5/3	75	S	sg	so po	lo	–	–	3f 3vf	–
Late Holocene Terrace	Platoro	A	0–15	10YR 3/2	10YR 4/3	<10	SiL	2 vf sbk	ss ps	fr	–	c s	3f 3vf	2f 3vf
		B1	15–41	10YR 3/2	10YR 4/3	<10	L	2 f sbk	ss ps	fr	–	c s	1m 2f 3vf	2m 2f 3vf
		B2	41–64	10YR 3/3	10YR 4/3	<10	L	2 f-m sbk	ss p	fr	–	a s	1f 3vf	2m 2f 3vf
		2C	64–93	10YR 3/2	10YR 5/3	50	LS	sg	so po	lo	–	–	–	–
Late Holocene Terrace	Lake Fork	A	0–11	10YR 3/2	10YR 4/2	<10	L	2 f gr	ss p	vfr-fr	–	c s	2f 3vf	3f 3vf
		AB	11–43	10YR 3/2	10YR 4/2	<10	L	2 f sbk	ss ps-p	fr	–	c s	1m 3f 3vf	2f 3vf
		B	43–62	10YR 2/2	10YR 4/3	<10	SL	2 f sbk	ss p	fi	–	g s	1f 1vf	1c 1m 2f 3vf
		2C	62–89	10YR 2/2	10YR 5/3	50	LS	sg	so po	lo	–	–	2f 2vf	–
Late Holocene Terrace	South Fork	A	0–20	7.5YR 3/2	10YR 5/2	<10	SiL	2 vf gr	ss p	vfr	–	a s	1m 3f 3vf	2m 3f 3vf
		Bw	20–27	10YR 4/2	10YR 5/3	<10	SL	2 f sbk	ss-sps	vfr-fr	–	a s	3f 3vf	2f 3vf
		C	27–37	10YR 3/2	10YR 4/3	<10	LS	sg	so po	lo	–	c s	1f 3vf	–
		2C	37–105	10YR 3/2	10YR 5/3	50–75	S	sg	so po	lo	–	–	1f 1vf	–
Late Holocene Terrace	Three Forks	Aw	0–13	10YR 3/3	10YR 5/4–5/6	<10	L	1.5 f-m sbk	vfr	ss-ps	–	c s	3m 3f 3vf	1f 1vf
		AB	13–20	10YR 3/4	10YR 4/3	<5	SL-L	1.5 c-m-f pl & abk	vfr & fi-vfi	ss ps	–	aw	3m 1f 1vf	1vf
		Ab	20–26	10YR 3/3	10YR 4/2	25	L	2 f-m-c abk	fr	ss ps	–	c s	1m 2f 2vf	2f 1vf
		ABb	26–36	10YR 4/3	10YR 5/3	10	SL-L	2 c-m-f abk	vfr	ss ps	–	a s	1m 1f 1 vf	3f 3vf
		B	36–64	10YR 3/3	10YR 3/3	<10	SL-L	2 c-m-f abk	fr	ss p	–	–	1f 1vf	3f 3vf
Late Holocene Terrace	Three Forks	A	0–5	10YR 3/3	10YR 6/2	40	SL	1 c-m sbk	vfr-fr	so po	–	c s	1m 3f 3vf	–
		Aw	5–31	10YR 3/2	10YR 6/1	50	S	sg-1 f-m gr-sbk	vf-lo	so po	–	g s	2f 3vf	–
		B1	31–36	10YR 3/4	–	0	L	2 f-m-c abk	fr	ss p	–	a s	2f 2vf	1f 3vf
		B2	36–61	10YR 3/4	–	30	L	2 f-m-c abk	fr	s p	–	c s	2c 1m 1f 1vf	1f 3vf
		B3	61–87	10YR 3/3	–	40	L	2 m-c abk	fr	ss ps	–	–	3m 1f 1vf	1 vf

(*continued*)

			Depth	Color		Gravel			Consistence		Clay			
Unit	Locality	Horizon	(cm)	Moist	Dry	(%)	Texture	Structure	Wet	Moist	Films	Boundary	Roots	Pores
Late Holocene Terrace	Middle Fork	A	0–10	10YR 3/3	10YR 5/4	25	L	1 m-f sbk	fr	ss ps	–	c s	1m 3f 3vf	–
		AB	10–25	10YR 3/3	10YR 6/3	10	L	1 f-m-c sbk	fr vfr	ss ps	–	c s	3f 3vf	1f 1vf
		B	25–45	10YR 4/4	10YR 4/3	10	L	2 f-m-c sbk	fr-vfr	ss ps	–	c w	2f 3vf	1f 3vf
		Ab	45–55	10YR 3/3	10YR 6/3	<10	L	2 f-m-c abk	fr	s ps	–	c s	1f 2vf	2f 3vf
		Bb1	55–95	10YR 3/4	10YR 5/6	>75	S	sg-1 f gr-sbk	vfr-fr	so po	–	a s	2vf	–
		Bb2	95–120	10YR 5/4	10YR 5/4	<10	SlL	2.5 m-c abk	fr-fi	s ps	–	–	–	1.5f 3vf
Mid Holocene Terrace	Platoro	AB	0–30	10YR 3/2	10YR 4/3	<10	L	2 m gr	ss ps	fr	–	c s	1m 3f 3vf	2f 3vf
		B	30–48	10YR 3/3	10YR 4/3	<10	L	2 f sbk	ss ps	fr	–	g s	3f 3vf	2f 3vf
		2C	48–94	10YR 3/3	10YR 5/3	50	S	sg	so po	lo	–	–	1m 2f 2vf	–
Mid Holocene Terrace	Lake Fork	A	0–22	10YR 3/2	10YR 4/3	<10	SiL	2 m gr	s p	fr	–	a s	2f 3vf	1m 1f 2vf
		Bt	22–38	10YR 4/3	10YR 4/4	<10	SiL	2 f abk	s p	fr	–	g s	1f 3vf	1m 1f 3vf
		2C	38–78	10YR 2/2	10YR 5/6	75	LS	sg	so po	lo	–	–	3f 3vf	–
Early Holocene Terrace	Platoro	A	0–15	10YR 2/2	10YR 4/2	<10	SiL	2 m gr	ss-s ps	fr	–	c s	2f 3vf	2f 3vf
		B	15–30	10YR 2/2	10YR 4/3	<10	SiL	2 f sbk	ss ps	fr	–	a s	1f 3vf	3f 3vf
		2BC	30–42	10YR 2/2	10YR 5/3	50–75	LS	2 f gr	so po	fr	–	a s	2f 3vf	1m 3f 3vf
		2C	42–80	10YR 2/2	10YR 5/3	75	LS	sg	so po	lo	–	–	3vf	–
Early Holocene Terrace	Lake Fork	A	0–18	10YR 3/2	10YR 4/3	10	SiL	2 m gr	s p	vfr	–	a s	2m 2f 3vf	1m 1f 3vf
		Bt	18–39	10YR 3/2	10YR 4/4	10	L	2 f abk	s p-vp	fr	–	g s	2f 2vf	2m 2f 3vf
		2C	39–80	10YR 2/2	10YR 5/6	50–75	SL	sg	so po	lo	–	–	1m 2f 2vf	–
Early Holocene Terrace	South Fork	A	0–9	10YR 2/2	10YR 4/2	<10	SiL	2 f gr	ss p	fr	–	a s	1f 3vf	1f 2vf
		Bt1	9–27	10YR 2/2	10YR 4/3	<10	SiL	2 m abk	s p	fi	–	a s	1f 3vf	2m 1f 3vf
		Bt2	27–37	10YR 4/3	10YR 4/4	<10	L	2 m abk	s p-vp	fi	–	c s	2vf	1m 1f 3vf
		2BtC	37–50	10YR 4/3	10YR 4/4	>75	SL	2 f abk	s p-vp	fr	–	a s	3vf	1f 3vf
		2C	50–78	10YR 2/2	10YR 4/4	>75	SL	sg	so po	lo	–	–	1f 2vf	–
Outwash Terrace	Platoro	A	0–20	10YR 2/2	10YR 4/2	<10	SiL	2 f sbk	ss-s ps	fr	–	a s	1m 3f 3vf	2f 2vf
		Bt	20–44	7.5YR 3/3	10YR 5/4	10–25	L	2 f sbk	ss-s p	fr	–	c s	3f 3vf	1m 2f 3vf
		2C	44–83	10YR 4/2	10YR 5/3	>75	S	sg	so po	lo	–	–	1f 2vf	–
Outwash Terrace	Lake Fork	A	0–12	10YR 2/2	10YR 4/2	<10	SiL	2 f sbk	ss p	fr	–	a s	2f 2vf	3f 3vf
		Bt	12–25	10YR 2/2	10YR 4/2	10	SiL	2 m abk	ss p	fr-fi	–	a s	2f 3vf	1f 1vf
		2B	25–70	10YR 4/3	10YR 5/3	50–75	L	2 f gr	ss-s ps-p	fr	–	–	1m 3f 3vf	1f 2vf
Outwash Terrace	Adams Fork	A	0–10.5	10YR 4/2	10YR 4/4	<10	L	1.5 c-m-f sbk	fr	ss ps	–	c s	m3 f. vf3	–
		AB	10.5–21.5	10YR 4/2	10YR 5/4	15	L	1.5 f-m-c sbk	fr-vfr	ss ps	–	g s	m3 f. vf3	1f
		B1	21.5–42	10YR 3/3	10YR 5/6	65	LS	1 m-c abk	vfr	ss po	–	c w	vf3 f. m1	1f vf1
		B2	42–57	10YR 3/3	10YR 5/3	70	LS	1-sg f g-sbk	fr-vfr	ss po	–	a s	f1 vf2	vf2 f1
		BC	57–102	10YR 3/4	10YR 5/4	70	S	sg g	lo	so po	–	–	vf1	vf1

(*continued on next page*)

(*continued*)

			Depth	Color		Gravel			Consistence		Clay			
Unit	Locality	Horizon	(cm)	Moist	Dry	(%)	Texture	Structure	Wet	Moist	Films	Boundary	Roots	Pores
Late Holocene Fan	Platoro	AB	0–34	10YR 3/1	10YR 4/2	<10	L	2 f sbk	ss ps	fr	–	c s	3f 3vf	3f 3vf
		B	34–84	10YR 3/2	10YR 5/2	<10	L	2 m sbk	s ps-p	fr	–	a s	1f 1vf	2m 2f 2vf
		2B	84–108	10YR 3/2	10YR 5/2	50	SL	2 f sbk	s p	fr	–	–	–	2f 3vf
Late Holocene Fan	South Fork	A	0–15	10YR 2/1	10YR 4/1	<10	L	2 f gr	s ps	fr	–	a s	1m 3f 3vf	2f 2vf
		AB	15–33	10YR 2/2	10YR 3/2	<10	L	2 f sbk	s ps	fi	–	a s	2m 2f 2vf	2m 3f 3vf
		Bw	33–65	7.5YR 2.5/2	10YR 4/2	<10	SL	2 f sbk	ss ps	vfr	–	a s	1m 1f 1vf	3m 1f 3vf
		Ab	65–72	10YR 2/1	10YR 3/1	<10	L	2 f abk	s ps	fi	–	a s	1vf	1m 2f 1vf
		Bb	72–85	7.5YR 2.5/2	10YR 4/2	<10	L	2 m sbk	ss p	fi	–	–	1vf	1f 2vf
Late Holocene Fan	Middle Fork	A	0–8	10YR 2/2	10YR 3/2	<5	L	sg-1 f-m sbk	vfr	ss ps	–	c s	3m 2f 3vf	–
		ABoxw	8–18	10YR 3/3	10YR 5/4	50	SL	sg-1 f sbk	vfr	so po	–	c s	2m 2f 3vf	–
		ABw	18–29	10YR 3/2	10YR 6/3	50	LS	1 f-m sbk	lo-vfr	so po	–	c s	1c 1m 2f 2vf	–
		C1	29–59	10YR 3/2	10YR 5/3	>75	LS	sg-1 f gr-sbk	lo-vfr	so po	–	g s	1m 3f 3vf	–
		C2	59–98	10YR 2/2	10YR 5/3	75	LS	sg-1 f-m abk-sbk	lo-vfr	so po	–	–	1m 1f 1vf	–
Late Holocene Fan	Upper Trunk Valley	A	0–12.5	10YR 3/2	10YR 4/4	10	L	1 f-m sbk	vfr-fr	ss ps	–	c s	2m 3f 3vf	1vf
		AB	12.5–28	10YR 3/2	10YR 5/3	25	L	1.5 vc-c-m-f abk-sbk	fr	ss ps	–	c s	2f 3vf	2f 1vf
		B1	28–41	10YR 3/3	10YR 5/2	10	L	2 vc-c-m-f sbk	fr	ss ps	–	c s	1vf	1f 3vf
		B2	41–58	10YR 2/2	10YR 5/3	40	L	2 f-m-c abk	fr	ss ps	–	c s	1vf	2f 3vf
		BC1	58–70	10YR 3/3	10YR 5/4	50	SL	1 f sbk	lo	ss po	–	c s	–	–
		BC2	70–80	10YR 3/3	10YR 6/4	45	LS-SL	1 f-m sbk	lo	so po	–	–	–	–
Late Holocene Fan	Upper Trunk Valley	ABw	0–39	10YR 4/2	10YR 4/3	40	SL	1 & 2 f & c gr & sbk	fr	s po-ps	–	c s	1m 3f 3vf	1f 3vf
		Bw	39–56	10YR 4/2	10YR 5/3	25	SL	2 f-m sbk	vfr	ss po	–	c s	2m 1f 1 vf	1f 3vf
		ABb	56–75	10YR 4/2	10YR 4/4	25	L		fr	s p	–	a w	3m 2f 2vf	1f 3vf
		C	75–100	10YR 4/3	10YR 5/3	75	SL	3 c abk	vfr	ss ps	–	–	2f 2vf	–
Mid Holocene Fan	Upper Trunk Valley	Aw	0–7	10YR 3/3	10YR 4/4	50	SL-L	1 f-m gr-sbk	lo-vfr	ss po	–	c s	3f 3vf	–
		Bw	7–23	10YR 3/2	10YR 6/5	25	SL-L	sg gr	lo	ss po	–	c s	1m 3f 3vf	–
		Ab	23–40	10YR 3/2	10YR 4/3	35	L	2 f-m-c abk	vfr	s p	–	a s	1m 3f 3vf	2f 2vf
		Bb1	40–56	10YR 3/3	10YR 5/2	30	L	2 f-m-c abk	fr	s p	–	c w	2f 2vf	3m 3f 3vf
		Bb2	56–85	10YR 4/3	10YR 5/3	25	L	2 f-m-c abk-sbk	fr	s ps	–	c s	1m 1f 1vf	3f 3vf
		Bb3	85–110	10YR 2/3	10YR 6/3	25	L	2 f-m abk	fr-vfr	s p	–	c s	2m 1f 1vf	1m 3f 3vf
		Bb4	110–130	10YR 4/3	10YR 6/3	45	L	2 f-m sbk	vfr	s p	–	–	1f 2vf	1m 3f 3vf
Early Holocene Fan	Platoro	A	0–9	10YR 2/1	10YR 3/1	<10	L	2 m gr	ss p	vfr	–	a w	3f 3vf	2f 3vf
		Bt	9–20	10YR 4/1	10YR 6/2	0	SiL	3 m abk	vs vp	fi	2 p pf	a w	2m 1f 2vf	2m 2f 2vf
		Ab	20–31	10YR 2/1	10YR 3/1	0	L	2 f sbk	ss ps	fr	–	a s	2m 2f 1vf	1m 2f 1vf
		Btb	31–41	10YR 3/1	10YR 5/1	0	SiCL	3 m sbk	vs vp	fi	3 p pf	c s	2m 2f	2m 2f 2vf
		C	41–82	10YR 4/2	10YR 6/2	<10	SL	sg	so po	lo	–	–	1f	–

(*continued*)

Unit	Locality	Horizon	Depth	Color		Gravel			Consistence		Clay			
			(cm)	Moist	Dry	(%)	Texture	Structure	Wet	Moist	Films	Boundary	Roots	Pores
Early Holocene Fan	Lake Fork	A	0–8	10YR 3/2	10YR 4/2	0	SiL	2 m gr	s ps	vfr-fr	–	a s	2m 3f 3vf	2f 3vf
		B	8–27	10YR 4/2	10YR 5/3	<10	L	2 f abk	vs p	fr	–	a s	1m 3f 3vf	1m 2f 3vf
		Ab	27–39	10YR 2/2	10YR 4/2	0	SiL	2 vf sbk	s p	vfr-fr	–	a s	1m 2f 2vf	2m 2f 3vf
		Btb	39–78	10YR 3/2	10YR 5/3	0	SiL	3 f abk	vs vp	fr	3 d cobr	–	1f 1vf	1m 2f 3vf
Early Holocene Fan	South Fork	A	0–18	10YR 2/1	10YR 3/2	<10	SiL	2 f gr	s ps	vfr	–	a s	2f 3vf	1f 2vf
		Bt1	18–41	10YR 4/2	10YR 5/3	10–25	L	2 vf abk	vs vp	fr-fi	3 d cobr	c s	2f 2vf	2m 2f 2vf
		Bt2	41–54	10YR 4/3	10YR 5/3	25	L	3 f abk	vs vp	fr-fi	3 d cobr	g s	2vf	1m 2f 3vf
		Bt3	54–81	10YR 4/3	10YR 5/3	<10	L	3 m abk	vs vp	fr-fi	3 d cobr	–	1vf	2m 3vf
Pleistocene-Holocene Fan	Upper Trunk Valley	AC	0–15	10YR 3/2	10YR 4/3	25	L	1 & 2 c-m-f gr	vfr	ss ps	–	c s	1m 3f 3vf	1f 2vf
		AB1	15–31	10YR 3/2	10YR 4/2	15	L	1 & 2 c-m-f sbk	vfr	ss ps	–	c s	1m 3f3vf	3m 3f 3vf
		AB2	31–57	10YR 3/2	10YR 4/2	10	L	2 vc-c-m sbk	vfr	ss p	–	c s	3f 3vf	1m 2f 2vf
		AB3	57–71	10YR 4/2	10YR 5/4	35	L	2 c-m sbk	fr-vfr	s p	–	g s	1f 1vf	1c 1m 1f 3vf
		AB4	71–83	10YR 3/3	10YR 5/3	<10	L	2 c-m abk	fr-vfr	s p	–	c s	1f 1vf	1m 1f 3vf
		AB5	83–111	10YR 4/2	10YR 4/3	10	L	2 c-m abk	fr-vfr	s p	–	c s	1f 1vf	3f 3vf
		Bw1	111–125	10YR 4/2	10YR 5/3	25	L	2 c-m abk	fr-vfr	s ps	–	a s	1f 1vf	1f 3vf
		Bw2	125–150	10YR 4/4	10YR 5/3	–	SL	c-m abk	vfr	ss ps	–	–	–	3f 3vf
Pleistocene-Holocene Fan	Upper Trunk Valley	O	0–1	–	10YR 2/2	–	–	–	–	–	–	a s	1m 3f 3vf	–
		A	1–9	10YR 3/2	10YR 5/4	<5	SlL	1 c-m-f sbk	vfr-fr	ss ps	–	c s	1c 3m 3f 3vf	1vf
		AB	9–16	10YR 3/3	10YR 4/3	<10	SlL	1 m-f abk-sbk	vfr-fr	ss ps	–	c s	2c 3m 3f 3vf	1f
		Box	16–32	10YR 4/4	10YR 6/6	70	L	1 vf-f sbk	vfr-fr	s ps	–	c s	1c 1m 3f 3vf	1m 1f 2vf
		B1 (Ab?)	32–43	10YR 4/3	10YR 4/3	50	L	1 f-m sbk	vfr-fr	s ps	–	c s	1m 3f 3vf	2m 2vf
		B2 (Bb?)	43–85	10YR 4/3	10YR 3/4	10	SlCL	2 f-m-c abk	vfr-fr	s p	–	–	2m 1f 1vf	2m 3f 3vf
Colluvium	Adams Fork	A	0–16.5	10YR 4/2	10YR 5/3	25	L	1.5 f-m-c sbk	fr	ss ps	–	c s	2m 3f 3vf	1f 1vf
		AB	16.5–26	10YR 4/3	10YR 5/3	25	L	1.5 f-m-c sbk	vfr-fr	ss ps	–	g s	1m 2f 3vf	3f 3vf
		B1	26–40	10YR 4/3	10YR 5/4	25	L	1.5 f-m-c abk	vfr-fr	ss ps	–	c s	1m 2f 2vf	2f 3vf
		B2	40–55	10YR 4/4	10YR 5/6	50	CL	2 f-m-c abk	vfr	s p	–	c s	1c 1m 1f 3vf	3f 3vf
		BC1	55–90	10YR 4/4	10YR 4/6	60	CL	2 f-m-c abk	vfr	s p	–	c s	2m 1f 1vf	3f 3vf
		BC2	90–120	10YR 4/4	10YR 6/3	65	SCL	1.5 f-m sbk	vfr	s p	–	–	–	3f 3vf
Colluvium	Adams Fork	A	0–21	10YR 3/2	–	<5	L	2 m-f-vf abk	fr	ss ps	–	c s	2vc 2c 3m 3f 3vf	1c 2m 1f 2vf
		AB1	21–38.5	10YR 3/2	–	<5	L	2 c-m-f-vf abk	fr	ss ps	–	g s	2c 3c 3m 3f 3vf	1c 3m 1f 3vf
		AB2	38.5–56	10YR 3/4	–	<5	L	2 c abk	fr	s p	–	c s	2c 2m 3f 3vf	1f 3vf
		Box	56–77.5	10YR 4/6	–	<1	L	2 c-m-f-vf abk	fr	ss ps	–	c s	2m 1f	3f 3vf
		B	77.5–89	10YR 4/6	–	<5	L	2 c-m-f-vf abk	fr	ss ps	–	a s	1m 1f	1m 3f 3vf
		C	89+	10YR 3/3	–	70	LS	1 m-f gr	vfr	so po	–	–	1f 2vf	1f 1vf

(*continued on next page*)

(*continued*)

			Depth	Color		Gravel			Consistence		Clay			
Unit	Locality	Horizon	(cm)	Moist	Dry	(%)	Texture	Structure	Wet	Moist	Films	Boundary	Roots	Pores
Colluvium	Upper Trunk Valley	A	0–8	2.5 Y 3/2	2.5 Y 4/2	<10	SlL	2 f abk	–	ss ps	–	c s	3f 3vf	1f 2vf
		AB	8–24	10YR 3/2	10YR 4/3	10	SCL	1.5 f-m-c abk	vfr-fr	s ps	–	c l	1m 1f 3vf	1vf
		B1	24–39	2.5 Y 4/3	2.5 Y 6/3	0	SlL	2 f-m abk	vfr-fr	s ps	–	c s	1f 2vf	1f 2vf
		B2	39–62	2.5 Y 5/3	2.5 Y 6/4	15	SlL	2 f-m abk	vfr-fr	ss ps	–	c w	1f 1vf	1f 1vf
		Cr	62–85	2.5 Y 4/3	2.5 Y 6/3	<10	L	2 m-c abk	fi-vfi	ss ps	–	–	1m 1f 1vf	–
Colluvium	Platoro	AB1	0–20	10YR 2/1	10YR 3/2	<10	SiL	2 f gr	ss ps	fr	–	g s	2f 3vf	2f 3vf
		AB2	20–40	10YR 2/1	10YR 4/2	25	SiL	2 f sbk	ss-s ps	fr	–	a s	2m 2f 3vf	1f 3vf
		Bw1	40–51	10YR 3/3	10YR 4/2	25–50	SL	2 vf sbk	ss po	fr	–	g s	1m 2f 2vf	2f 3vf
		Bw2	51–90	10YR 4/3	10YR 5/3	75	SL	2 vf sbk	s ps	fr	–	–	2f 1vf	1m 3f 3vf
Colluvium	South Fork	A	0–14	10YR 2/2	10YR 4/2	10–25	SiL	2 m gr	s p	fr	–	a s	2m 3f 3vf	1f 3vf
		AB	14–29	10YR 2/2	10YR 3/2	10	SiL	2 f sbk	s p	fr	–	a s	1c 2m 3f 3vf	1m 1f 3vf
		Bt1	29–42	7.5YR 4/2	7.5YR 4/3	10	CL	3 f abk	vs p	fr-fi	3 d cobr	–	1c 1m 1f 1vf	3m 1f 1vf
		Bt2	42–65	7.5YR 4/3	7.5YR 4/3	50	CL	3 m abk	vs vp	fi	3 d cobr	–	1m 2f 1vf	2m 2vf
Glacial Till	Adams Fork	A	0–33.5	10YR 3/2	10YR 4/3	10	SL	1 & 2 m & c sbk	vfr-fr	ss-po	–	g s	2m 3f 3vf	1f 1vf
		A/Box	33.5–76	10YR 3/3	10YR 3/3	50	SL	1 m-c sbk	vfr	ss-po	–	c s	1m 2f 2vf	1f 1vf
		Box	see above	10YR 3/3	10YR 5/4	50	SL	1–2 m-c abk	vfr	ss-po	–	a b	2f 1vf	1f 2vf
		C	76–120	10YR 3/3	10YR 7/4	75	SL	sg	lo	ss po	–	–	1f 1vf	–
Glacial Till	Upper Trunk Valley	A	0–14	10YR 3/1	10YR 3/2	<1	L	2 m-c sbk	fr	s p	–	c s	1m 3f 3vf	2m 3f 3vf
		AB	14–28	10YR 3/2	10YR 4/2	<5	L	2 m-c sbk	vfr	s ps	–	a s	1m 3f 3vf	2m 3f 3vf
		Bw	28–51	10YR 3/2	–	60	SLC-L	1 f0m0c abk	fr	s ps	–	c s	1m 2f 3vf	1m 3f 3vf
		Box	51–?	10YR 3/4	10YR 5/4	40	SCL	1 m-f sbk	vfr-fr	s p	–	–	1m 2f 2vf	–
Glacial Till Glacial Till	North Fork	A	0–15	10YR 4/3	10YR 5/4	<10	L	1.5 f-m-c sbk	fr-vfr	ss ps	–	c s	2m 3f 3vf	1vf
		AB	15–54	10YR 3/3	10YR 5/4	<10	L	2 c-m-f sbk	vfr	ss ps	–	a s	1m 2f 2vf	1m 2f 3vf
		Bw1	54–65	10YR 4/4	10YR 7/4	40	L	2 m-f abk	fr-vfr	s ps	–	a w	1f 1 vf	1f 3vf
		Bw2	65–79	10YR 3/6	10YR 6/4	35	LS	1 m-f-sbk	vfr	so po	–	a w	1f 1 vf	1f 3vf
		C	79–90	10YR 4/4	10YR 6/3	>75	S	sg gr	lo	so po	–	–	–	–
	Middle Fork	AB	0–17	10YR 3/3	–	35	L	1.5 m-c sbk	vfr-fr	ss ps	–	c s	3m 3f 3vf	–
		Bw1	17–30	10YR 3/3	–	25	L	1.5 c-m-f sbk	vfr-fr	ss ps	–	c s	3m 3 f 2vf	2f 3vf
		Bw2	30–44	10YR 3/4	–	15	L	2 m-c-vc abk-sbk	vfr-fr	ss ps	–	g s	2m 3f 1vf	1m 2f 3vf
		Bw3	44–60	10YR 4/3	–	35	L	2 f-m-c abk-sbk	vfr-fr	ss ps	–	g s	3m 1f 1 vf	1m 1f 3vf
		Bw4	60–86	10YR 3/3	–	35	L	2 m-c pl-abk	fr	ss ps	–	–	2m 1f 1vf	1m 2f 3vf
Glacial Moraine	Terrace Reservoir	A	0–18	10YR 3/2	10YR 4/2	35	L	2 c-m-f sbk	–	ss ps	–	c w	3m 2f 2vf	3vf
		Bw1	18–35	10YR 4/2	10YR 4/3	25	SCL	2 v-m abk	–	s-vs p	–	c w	3m 2f 2vf	1vf
		Bw2	35–50	10YR 5/3	10YR 4/4	30	SCL	2 f-m abk	–	s-vs p	–	c s	2m 2f 2vf	2f 3vf
		Bw3	50–80	10YR 5/2	10YR 5/4	75	SlL	1 f-m abk	–	s ps	–	c s	2m 1f 1vf	–
		BC	80–115	10YR 5/3	10YR 4/3	90	SCL	sg-1 f-fr-sbk	–	s p	–	c w	1m 1f 1vf	–
		C	115–160	10YR 5/4	10YR 6/3	>75	LS	sg gr	–	so po	–	–	1m 1f 1vf	–

(*continued*)

Unit	Locality	Horizon	Depth (cm)	Color Moist	Color Dry	Gravel (%)	Gravel Texture	Gravel Structure	Consistence Wet	Consistence Moist	Clay Films	Clay Boundary	Clay Roots	Clay Pores
Glacial Moraine	Cumbres Bog	A	0–17	10YR 3/2	10YR 4/2	50	L	1 f sbk	vfr	ss ps	–	c s	1m 3f 3vf	–
		AB	17–27	10YR 3/3	10YR 5/3	40	SL	2 f-m abk	vfr	ss ps	–	c s	2m 1f 3vf	2f 3vf
		Bw1	27–49	7.5YR 4/4	10YR 5/4	40	SCL	2 m-c abk	fr	s ps	–	g s	2m 1f 3vf	2f 1vf
		Bw2	49–74	7.5YR 4/3	10YR 7/4	35	SCL	2 f-m-c abk	fr	s ps	–	g s	2m 1f 1vf	3f 3vf
		Bw3	74–89	7.5YR 5/4	10YR 6/4	50	SCL	2 f-m-c abk	fr	s ps	–	c s	1f 1vf	3f 3vf
		BC	89–100	7.5YR 5/4	10YR 5/4	50	SCL	sg-1 f-m sbk	lo-vfr	s ps	–	–	–	–

Texture	Structure 1	Structure 2	Structure 3	Clay films 1	Clay films 2	Clay films 3
C — clay	1 — few	f — fine	abk — angular blocks	1 — few	f — faint	pf — ped faces
CL — clay loam	2 — common	m — medium	sbk — subangular blocks	2 — common	d — distinct	po — pores
SiCL — silty clay loam	3 — many	c — coarse	pl — plates	3 — many	p — prominent	br — bridges
SiC — silty clay	m — massive					co — coats
L — loam	sg — single grain	Moist consistency	Wet consistency	Boundaries	Roots and pores	
SiL — silty loam		lo — loose	so — non sticky	a — abrupt	1 — few	
SL — sandy loam		fr — friable	po — non plastic	c — clear	2 — common	
LS — loamy sand		fi — firm	ss — slightly sticky	g — gradual	3 — many	
S — sand		vfi — very firm	ps — slightly plastic	d — diffuse	vf — very fine	
		efi — extremely firm	p — plastic	s — smooth	f — fine	
			vs — very sticky	w — wavy	m — medium	
			vp — very plastic	l — irregular	c — coarse	
				b — broken		

References

Adams, D.K., Comrie, A.C., 1997. The North American monsoon. Bull. Am. Meteorol. Soc. 78, 2197.

Anderson, S.P., Anderson, R.S., Hinckley, E.S., Kelly, P., Blum, A., 2011. Exploring weathering and regolith transport controls on critical zone development with models and natural experiments. Appl. Geochem. 26, S3–S5 (Supplement).

Ariztegui, D., Bösch, P., Davaud, E., 2007. Dominant ENSO frequencies during the Little Ice Age in Northern Patagonia: the varved record of proglacial Lago Frías, Argentina. Quat. Int. 161, 46–55.

Atwood, W.W., Mather, K.F., 1932. Physiography and Quaternary geology of the San Juan Mountains, Colorado. U.S. Geol. Surv. Prof. Pap. 166, 1–176.

Bain, D.C., Mellor, A., Robertson-Rintoul, M.S.E., Buckland, S.T., 1993. Variations in weathering processes and rates with time in a chronosequence of soils from Glen Feshie, Scotland. Geoderma 57, 275–293.

Berry, M.E., 1987. Morphological and chemical characteristics of soil catenas on pinedale and Bull Lake moraine slopes in the Salmon River Mountains, Idaho. Quat. Res. 28, 210–225.

Birkeland, P.W., 1984a. Soils and Geomorphology. 2nd ed. Oxford University Press, New York.

Birkeland, P.W., 1984b. Holocene soil chronofunctions, Southern Alps, New Zealand. Geoderma 34, 115–134.

Birkeland, P.W., 1999. Soils and Geomorphology. 3rd ed. Oxford University Press, New York.

Birkeland, P.W., Burke, R.M., 1988. Soil catena chronosequences on eastern Sierra Nevada moraines, California, U.S.A. Arct. Alp. Res. 20, 473–484.

Birkeland, P.W., Burke, R.M., Shroba, R.R., 1987. Holocene Alpine soils in gneissic cirque deposits, Colorado Front Range. USGS Geol. Surv. Bull. 1590-E, 1–20.

Birkeland, P.W., Burke, R.M., Benedict, J.B., 1989. Pedogenic gradients for iron and aluminum accumulation and phosphorus depletion in arctic and alpine soils as a function of time and climate. Quat. Res. 32, 193–204.

Birkeland, P.W., Shroba, R.R., Burns, S.F., Price, A.B., Tonkin, P.J., 2003. Integrating soils and geomorphology in mountains—an example from the Front Range of Colorado. Geomorphology 55, 329–344.

Carrara, P.E., Andrews, J.T., 1976. Holocene glacial/periglacial record; northern San Juan Mountains, Southwestern Colorado. Z. Gletscherk. Glazialgeol. 11, 155–174.

Carrara, P.E., Mode, W.N., Rubin, M., 1984. Deglaciation and postglacial timberline in the San Juan Mountains, Colorado. Quat. Res. 21, 42–55.

Carrara, P.E., Trimble, D.A., Rubin, M., 1991. Holocene treeline fluctuations in the northern San Juan Mountains, Colorado, U.S.A., as indicated by radiocarbon-dated conifer wood. Arct. Alp. Res. 23 (233–246), 233.

Deal, R.M., 2014. Temporal and Spatial Variability of Post-last Glacial Maximum (LGM) Climate Records Derived From Bog Cores, Southern San Juan Mountains, Colorado.

Dethier, D.P., Lazarus, E.D., 2006. Geomorphic inferences from regolith thickness, chemical denudation and CRN erosion rates near the glacial limit, Boulder Creek catchment and vicinity, Colorado. Geomorphology 75, 384–399.

Douglass, D., Mickelson, D., 2007. Soil development and glacial history, West Fork of Beaver Creek, Uinta Mountains, Utah. Arct. Antarct. Alp. Res. 39, 592–602.

Egli, M., Fitze, P., Mirabella, A., 2001a. Weathering and evolution of soils formed on granitic, glacial deposits: results from chronosequences of Swiss alpine environments. Catena 45, 19–47.

Egli, M., Mirabella, A., Fitze, P., 2001b. Clay mineral formation in soils of two different chronosequences in the Swiss Alps. Geoderma 104, 145–175.

Egli, M., Mirabella, A., Fitze, P., 2003a. Formation rates of smectites derived from two Holocene chronosequences in the Swiss Alps. Geoderma 117, 81–98.

Egli, M., Mirabella, A., Sartori, G., Fitze, P., 2003b. Weathering rates as a function of climate: results from a climosequence of the Val Genova (Trentino, Italian Alps). Geoderma 111, 99–121.

Engel, S.A., Gardner, T.W., Ciolkosz, E.J., 1996. Quaternary soil chronosequences on terraces of the Susquehanna river, Pennsylvania. Geomorphology 17, 273–294.

Eppes, M.C., McFadden, L., 2008. The influence of bedrock weathering on the response of drainage basins and associated alluvial fans to Holocene climates, San Bernardino Mountains, California, USA. The Holocene 18, 895–905.

Eppes, M.C., Bierma, R., Vinson, D., Pazzaglia, F.J., 2008. A soil chronosequence study of the Reno valley, Italy: insights into the relative role of climate versus anthropogenic forcing on hillslope processes during the mid-Holocene. Geoderma 147 (97–108), 97.

Evans, D.J.A., Benn, D.I., 2004. A Practical Guide to the Study of Glacial Sediments. p. 266.

Fall, P.L., 1997. Timberline fluctuations and late Quaternary paleoclimates in the southern Rocky Mountains, Colorado. Geol. Soc. Am. Bull. 109, 1306–1320.

Fortin, D., Langley, S., 2005. Formation and occurrence of biogenic iron-rich minerals. Earth Sci. Rev. 72, 1–19.

Gosse, J.C., Evenson, E.B., Klein, J., Lawn, B., Middleton, R., 1995. Precise cosmogenic ^{10}Be measurements in western North America: support for a global Younger Dryas cooling event. Geology 23, 877–880.

Guido, Z.S., Ward, D.J., Anderson, R.S., 2007. Pacing the post-last glacial maximum demise of the Animas Valley glacier and the San Juan Mountain ice cap, Colorado. Geology 35, 739–742.

Harden, J.W., 1982. A quantitative index of soil development from field descriptions: Examples from a chronosequence in central California. Geoderma 28, 1–28.

Haugland, J., Owen, B., 2005. Temporal and spatial variability of soil pH in patterned-ground chronosequences: Jotunheimen, Norway. Phys. Geogr. 26, 299–312.

Jiménez-Moreno, G., Fawcett, P.J., Scott Anderson, R., 2008. Millennial- and centennial-scale vegetation and climate changes during the late Pleistocene and Holocene from northern New Mexico (USA). Quat. Sci. Rev. 27, 1442–1452.

Johnson, B.G., Eppes, M.C., Diemer, J.A., 2010. Surficial geologic map of the upper Conejos River drainage, southeastern San Juan Mountains, southern Colorado. J. Maps v2010, 30–39.

Johnson, B.G., Eppes, M.C., Diemer, J.A., Jiménez-Moreno, G., Layzell, A.L., 2011. Post-glacial landscape response to climate variability in the southeastern San Juan Mountains of Colorado, USA. Quatern. Res. 76, 352–362.

Johnson, B.G., Jiménez-Moreno, G., Eppes, M.C., Diemer, J.A., Stone, J.R., 2013. A multi-proxy record of post-glacial climate variability from a shallowing, 12 m deep sub-

alpine bog in the southeastern San Juan Mountains of Colorado. The Holocene 23, 1028–1038.
Layzell, A.L., 2010. Soils and Geomorphology of Central Conejos River Valley: Fluvial Response to Post Last Glacial Maximum Climates and Sediment Supply (M.S.).
Layzell, A.L., Eppes, M.C., Johnson, B.G., Diemer, J.A., 2012a. Post-last glacial maximum range of variability in the Conejos River Valley, Southern Colorado: fluvial response to climate change and sediment supply. Earth Surf. Process. Landf. 37, 1189–1202.
Layzell, A.L., Eppes, M.C., Lewis, R.Q., 2012b. A soil chronosequence study on terraces of the Catawba River, near Charlotte, NC: insights into the long-term evolution of a major Atlantic Piedmont drainage basin. Southeast. Geol. 49.
Leigh, D.S., 1996. Soil chronosequence of brasstown creek, Blue Ridge mountains, USA. Catena 26, 99–114.
Leigh, D.S., Webb, P.A., 2006. Holocene erosion, sedimentation, and stratigraphy at Raven Fork, Southern Blue Ridge Mountains, USA. Geomorphology 78, 161–177.
Leopold, M., Völkel, J., Dethier, D., Huber, J., Steffens, M., 2011. Characteristics of a paleosol and its implication for the critical zone development, Rocky Mountain Front Range of Colorado, USA. Appl. Geochem. 26, S72–S75 (Supplement).
Lipman, P.W., 1974. Geologic Map of the Platoro Caldera Area, Southeastern San Juan Mountains, Southwestern Colorado.
Lipman, P.W., 1975a. Evolution of the Platoro caldera complex and related volcanic rocks, Southeastern San Juan Mountains, Colorado. USGS Professional Paper 852. U.S. Government Print Office, Washington.
Lipman, P.W., 1975b. Geologic map of the lower Conejos River Canyon area, southeastearn San Juan Mountains, Colorado.
Lipman, P.W., Steven, T.A., Mehnert, H.A., 1970. Volcanic history of the San Juan Mountains, Colorado, as indicated by potassium–argon dating. Geol. Soc. Am. Bull. 2329–2341, 2329.
McDonald, E.V., Busacca, A.J., 1990. Interaction between aggrading geomorphic surfaces and the formation of a late pleistocene paleosol in the Palouse loess of eastern Washington state. Geomorphology 3, 449–469.
McFadden, L.D., Hendricks, D.M., 1985. Changes in the content and composition of pedogenic iron oxyhydroxides in a chronosequence of soils in southern California. Quat. Res. 23, 189–204.
McFadden, L.D., McAuliffe, J.R., 1997. Lithologically influenced geomorphic responses to Holocene climatic changes in the Southern Colorado Plateau, Arizona: a soil-geomorphic and ecologic perspective. Geomorphology 19, 303–332.
McFadden, L.D., Weldon, R.J., 1987. Rates and processes of soil development on Quaternary terraces in Cajon Pass, California. Geol. Soc. Am. Bull. 98, 280–293.
McFadden, L.D., Ritter, J.B., Wells, S.G., 1989. Use of multiparameter relative-age methods for age estimation and correlation of alluvial fan surfaces on a desert piedmont, eastern Mojave Desert, California. Quatern. Res. 32, 276–290.
Mehra, O.P., Jackson, M.L., 1960. Iron oxide removal from soils and clays by a dithionite citrate system buffered with sodium bicarbonate. Clays Clay Minerals 7, 313–317.
Mellor, A., 1986. A micromorphological examination of two alpine soil chronosequences, Southern Norway. Geoderma 39, 41–57.
Mills, H.H., Allison, J.B., 1995. Weathering and soil development on fan surfaces as a function of height above modern drainageways, Roan Mountain, North Carolina. Geomorphology 14, 1–17.
Morgan, P., Seager, W., Golombek, M., 1986. Cenozoic thermal, mechanical and tectonic evolution of the Rio Grande Rift. J. Geophys. Res. 91 (B6), 6263–6276.
Pollack, J., Ciolkosz, E.J., Sevon, W.D., 2000. Pedogeomorphology in the Piedmont upland of Lancaster County, Pennsylvania. Southeast. Geol. 39.
Riggins, S.G., Anderson, R.S., Anderson, S.P., Tye, A.M., 2011. Solving a conundrum of a steady-state hilltop with variable soil depths and production rates, Bodmin Moor, UK. Geomorphology 128, 73–84.
Ritter, J.B., Miller, J.R., Enzel, Y., Howes, S.D., Nadon, G., Brubb, K.A., Hoover, K.A., Olsen, T., Reneau, S.L., Sack, D., Summa, C.L., Taylor, I., Touysinhthiphonexay, K.C.N., Yodis, E.G., Schneider, N.P., Ritter, D.F., Wells, S.G., 1993. Quaternary evolution of the Cedar Creek Alluvial Fan, Montana. Geomorphology 8, 287–304.
Schoeneberger, P.J., Wysocki, D.A., Benham, E.C., Broderson, W.D., 2002. Field Book for Describing and Sampling Soils: Version 2.0. Natural Resources Conservation Service, National Soil Survey Center, Lincoln, NE.
Schwertmann, U., Friedl, J., Stanjek, H., 1999. From Fe(III) ions to ferrihydrite and then to hematite. J. Colloid Interface Sci. 209, 215–223.
Shaw, J.N., Odom, J.W., Hajek, B.F., 2003. Soils on Quaternary terraces of the Tallapoosa River, Central Alabama. Soil Sci. 168.
Taylor, A., Blum, J.D., 1995. Relation between soil age and silicate weathering rates determined from the chemical evolution of a glacial chronosequence. Geology 23, 979–982.
Tsai, H., Hseu, Z., Huang, W., Chen, Z., 2007. Pedogenic approach to resolving the geomorphic evolution of the Pakua River terraces in central Taiwan. Geomorphology 83, 14–28.
Wells, S.G., McFadden, L.D., Dohrenwend, J.C., 1987. Influence of late Quaternary climatic change on geomorphic and pedogenic processes on a desert piedmont, eastern Mojave Desert, California. Quat. Res. 27, 130–146.